# BRIDGING THE SPECTRUM GAP: MID-FREQUENCY AUGMENTATION AND KEY-FREQUENCY MINING FOR MULTIVARIATE TIME SERIES

#### **Anonymous authors**

000

001

002

004

006

008 009 010

011 012 013

014

015

016

017

018

019

021

023

025

026

027

028

029

031 032 033

034

037

040

041

042

043

044

045

046

047

048

051

052

Paper under double-blind review

#### **ABSTRACT**

Recent advancements have progressively incorporated frequency-based techniques into deep learning models, leading to notable improvements in accuracy and efficiency for time series analysis tasks. However, the Mid-Frequency Spec**trum Gap** in the real-world time series, where the energy is concentrated at the low-frequency region while the middle-frequency band is negligible, hinders the ability of existing deep learning models to extract the crucial frequency information. Additionally, the shared **Key-Frequency** in multivariate time series, where different time series share indistinguishable frequency patterns, is rarely exploited by existing literature. This work bridges these two gaps by: (i) introducing a novel module, 'Adaptive Mid-Frequency Energy Optimizer', based on convolution and residual learning, to emphasize the significance of midfrequency bands; (ii) proposing an 'Energy-based Key-Frequency Picking Block' to capture shared Key-Frequency, which achieves superior inter-series modeling performance with fewer parameters; (iii) employing 'Key-Frequency Enhanced Training' strategy to further enhance Key-Frequency modeling, where spectral information from other channels is randomly introduced into each channel. Our approach advanced multivariate time series forecasting on the challenging Traffic, ECL, and Solar benchmarks, reducing MSE by 4%, 6%, and 5% compared to the previous SOTA iTransformer. Code is available at this **Anonymous Repo**: https://anonymous.4open.science/r/ReFocus-2889.

#### 1 Introduction

Accurate forecasting of time series offers reference for decision-making across various domains (Lim & Zohren, 2021; Torres et al., 2021), including weather (Du et al., 2023), economics (Oreshkin et al., 2020), and energy (Dong et al., 2023; Liu et al., 2022b). Especially, long-term multivariate time series forecasting (LMTSF) emerges as a prominent area of interest in academic research (Wang et al., 2024d; Wen et al., 2022) and industrial applications (Cirstea et al., 2022), offering the advantage of capturing complex interdependencies and trends across multiple variables.

Recently, the powerful representation capabilities of neural networks, such as Multi-Layer perception (MLPs) (Yi et al., 2023c; Han et al., 2024), Transformers (Zhou et al., 2022c; Nie et al., 2023), and Temporal Convolution Network (TCNs) (Eldele et al., 2024; Liu et al., 2022a), have significantly advanced deep learning-based LMTSF. These approaches can be broadly categorized into two/three folds: time-domain-based (Han et al., 2024; Nie et al., 2023; Liu et al., 2022a) and frequency-domain-based (Yi et al., 2023c; Zhou et al., 2022c; Eldele et al., 2024) methods, or mixed time & frequency. Time-domain methods are intuitive, handling nonlinearity and non-periodic signals directly from the raw sequence (Li et al., 2023) using Transformers (Zhou et al., 2022a), TCN (Donghao & Xue, 2024), or MLP (Wang et al., 2024a). The latest study Yi et al. (2024) highlights that time-domain forecasters face challenges such as vulnerability to high-frequency noise, and computational inefficiencies. While frequency-domain-based methods usually transform the time-domain data to the frequency spectrum by Fast Fourier transform (FFT) (Yi et al., 2023a). Then other operations (Self-attention (Zhou et al., 2022c), Linear mapping (Xu et al., 2024b; Yi et al., 2023c), etc.) are employed to extract frequency information. These methods benefit from advantages such as computational efficiency (Fan et al.,

2024; Xu et al., 2024b), periodic patterns extracting (Wu et al., 2023; Dai et al., 2024), and energy compaction (Yi et al., 2023c;b).

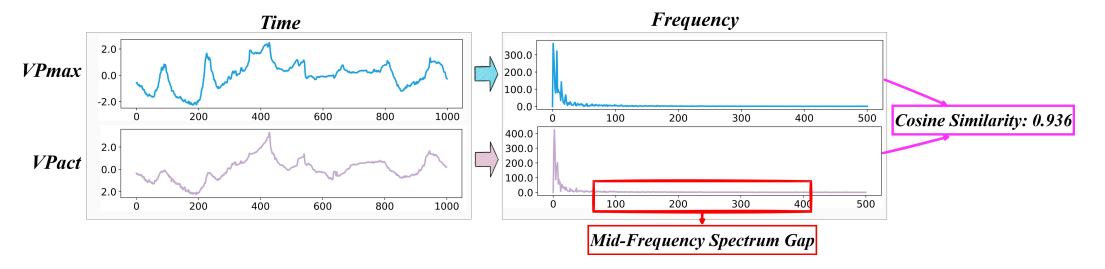


Figure 1: The **Mid-Frequency Spectrum Gap** and the shared **Key-Frequency** (high similarity in frequency spectra across variables) on Weather dataset. VPmax means 'Maximum Vapor Pressure' and VPact means 'Actual Vapor Pressure'.

However, existing frequency-domain-based forecasters usually face TWO significant challenges when dealing with real-world long-term time series: the **Mid-Frequency Spectrum Gap** and the shared **Key-Frequency modeling**.

- Mid-Frequency Spectrum Gap (Figure 1 Red box) refers to a condition where the energy of the spectrum is concentrated in the low-frequency regions, resulting in the mid-frequency band being negligible. Low-frequency components capture long-term trends, often contributing to mean shifts when overly concentrated (Stock & Watson, 2002; Granger & Newbold, 1974; Chatfield & Xing, 2019). So this Mid-Frequency Spectrum Gap will introduce Nonstationarity (Cheng et al., 2015; Liu et al., 2022c), where the mean and variance of time series change over time, and make time series less predictable. Furthermore, such uneven energy distribution challenges existing deep-learning models to extract critical patterns (Tishby & Zaslavsky, 2015; Xu et al., 2024a; Rahaman et al., 2019). So, addressing this Mid-Frequency Spectrum Gap is crucial for enhancing the feature extraction capabilities of deep learning-based forecasters (Park et al., 2019; Bai et al., 2018; Guo et al., 2019). Currently, widely used methods for processing spectra, such as Filters (Asselin, 1972), and **RevIN** (Kim et al., 2022; Liu et al., 2022c)—a technique previously applied to address nonstationarity—are not effective in resolving this issue. Conversely, convolution with residual connections has effectively handled spectral information (Can & Timofte, 2018; Chakraborty & Trehan, 2021), providing a potential solution.
- Meanwhile, the second challenge: the shared Key-Frequency Modeling (Figure 1 Pink box) has the disadvantage that distinct time series can exhibit indistinguishable frequency patterns, potentially leading to challenges in accurately differentiating and analyzing individual series within a multivariate context (Yu et al., 2023; Piao et al., 2024). However, existing approaches have largely overlooked this critical characteristic. Meanwhile, energy, which is the square of the amplitude of the spectrum, is proven as an effective tool for identifying certain frequency patterns in the multivariate case (Bógalo et al., 2024; Chekroun & Kondrashov, 2017; Sundararajan & Bruce, 2023).

Based on the above observations, this work mainly addresses two critical questions: (1) How can the Mid-Frequency Spectrum Gap be resolved to achieve a more evenly dispersed spectrum? (2) How can inter-series dependencies be efficiently modeled by leveraging the shared Key-Frequency? To tackle challenge 1, we propose the 'Adaptive Mid-Frequency Energy Optimizer' (AMEO), a convolution-and residual learning-based solution. It adaptively scales the frequency spectrum by assigning higher scaling factors to lower frequencies, thereby dispersing the spectrum. To address challenge 2, for the second challenge, we introduce the 'Energy-based Key-Frequency Picking Block (EKPB)', which features fewer parameters and faster inference speeds compared to the Transformer Encoder (Liu et al., 2024b) and MLP-Mixer (Chen et al., 2023). EKPB extracts shared frequency information across channels effectively. We also propose a 'Key-Frequency Enhanced Training' strategy (KET) which incorporates spectral information from other channels during training to enhance extraction of shared Key-Frequency that may not be included in the training set. We name our full framework ReFocus, (Residual Frequency Optimization and Cross-channel Unified Spectrum modeling), as it refocuses model capacity on underutilized yet critical spectral regions and inter-series frequency.

Our contributions are summarized as follows:

- We theoretically and empirically demonstrate that existing RevIN and high/low-pass filters
  fail to address the Mid-Frequency Spectrum Gap. We propose AMEO, a novel approach
  based on convolution and residual learning that significantly enhances mid-frequency feature
  extraction.
- We propose EKPB to capture shared Key-Frequency across channels, which achieves superior inter-series modeling capacity with lower parameters.
- We propose KET, where spectral information from other channels is randomly introduced into each channel, to enhance the extraction of the shared Key-Frequency.
- Our approach outperforms the previous SOTA iTransformer by reducing MSE by 4%, 6%, and 5% on the challenging Traffic, ECL, and Solar datasets, respectively, establishing new benchmarks in multivariate time series forecasting.

#### 2 Related work

Advancement in Recent Deep Learning-based Time Series Forecasting Recent advancements in deep learning-based time series forecasting can be broadly categorized into three key areas: (1) the application of sequential models to time series data, (2) the tokenization of time series, and (3) the exploration of intrinsic patterns within time series. Efforts in the first area have focused on deploying various architectures for time series forecasting, including Transformer (Wu et al., 2021; Wang et al., 2024b), Mamba (Ahamed & Cheng, 2024; Wang et al., 2024e), MLPs (Wang et al., 2024a; Das et al., 2023; Yu et al., 2024a), RNNs (Lin et al., 2023), Graph Neural Networks (Shang et al., 2024), TCNs (Wang et al., 2023), and even Large Language Models (LLMs) (Jin et al., 2024; Liu et al., 2024d;c). The second direction has witnessed groundbreaking developments, particularly in Patch Embedding (Nie et al., 2023) and Variate Embedding (Liu et al., 2024b). The final area explores modeling complex relationships, including the inter-series dependencies (Ng et al., 2022; Chen et al., 2024), the dynamic evolution within a sequence (Du et al., 2023; Zhang et al., 2022), or both (Yu et al., 2024b; Liu et al., 2024a).

**Time Series Modeling with Frequency** Frequency as a key feature of time series data, has inspired numerous works (Yi et al., 2023a). FITS (Xu et al., 2024b) employs a simple frequency-domain linear, getting results comparable to SOTA models with 10K parameters. Autoformer (Wu et al., 2021) introduces the auto-correlation mechanism, leveraging FFT to improve self-attention. FEDformer (Zhou et al., 2022c) further calculates attention weights from the spectrum of queries and keys. FiLM (Zhou et al., 2022b) applies Fourier analysis to preserve historical information while filtering out noise. FreTS (Yi et al., 2023c) incorporates frequency-domain MLP to model both channel and temporal dependencies. TimesNet (Wu et al., 2023) utilizes FFT to extract periodic patterns. FilterNet (Yi et al., 2024) proposes a filter-based method from the perspective of signal processing.

However, they do not address the Mid-Frequency Spectrum Gap and shared Key-Frequency modeling. In contrast, our method employs 'Adaptive Mid-Frequency Energy Optimizer' to improve mid-frequency feature extraction and introduces 'Energy-based Key-Frequency Picking Block' with 'Key-Frequency Enhanced Training' strategy to capture shared Key-Frequency across channels.

# 3 METHODOLOGY

# 3.1 PROBLEM DEFINITION

Given a multivariate time series input  $X \in \mathbb{R}^{C \times T}$ , multivariate time series forecasting tasks are designed to predict its future F time steps  $Y \in \mathbb{R}^{C \times F}$  using past T steps. C is the number of variates or channels.

#### 3.2 Preliminary Analysis

This section presents why RevIN (Kim et al., 2022; Liu et al., 2022c), High-pass, and Low-pass filters fail to address the Mid-Frequency Spectrum Gap. Let the input univariate time series be x(t) with length T and target y(t) with length F.

**Definition 3.1** (Frequency Spectral Energy). The Fourier transform of x(t), X(f), and its spectral energy  $E_X(f)$  is given by:

$$X(f) = \sum_{t=0}^{T-1} x(t)e^{-i2\pi ft/T-1}, \quad f = 0, 1, \dots, T-1$$
$$E_X(f) = |X(f)|^2. \tag{1}$$

## Impact of RevIN on Frequency Spectrum

**Definition 3.2** (Reversible Instance Normalization). Given a **forecast model**  $f : \mathbb{R}^T \to \mathbb{R}^F$  that generates a forecast  $\hat{y}(t)$  from a given input x(t), RevIN is defined as:

$$\hat{x}(t) = \frac{x(t) - \mu}{\sigma}, \quad t = 0, 1, \dots, T - 1$$

$$\hat{y}(t) = f(\hat{x}(t)), \quad \hat{y}(t)_{rev} = \hat{y}(t) \cdot \sigma + \mu,$$

$$\mu = \frac{1}{T} \sum_{t=0}^{T-1} x(t), \quad \sigma = \sqrt{\frac{1}{T} \sum_{t=0}^{T-1} (x(t) - \mu)^2}.$$
(2)

**Theorem 3.3** (Frequency Spectrum after RevIN). *The spectral energy of*  $\hat{x}(t)$  (transformed using RevIN):

$$E_{\hat{X}}(0) = 0, \quad f = 0,$$
  
 $E_{\hat{X}}(f) = \left(\frac{1}{\sigma}\right)^2 |X(f)|^2, \quad f = 1, 2, \dots, T - 1.$  (3)

The proof is in Appendix A.1. Theorem 3.3 suggests that RevIN scales the absolute spectral energy by  $\sigma^2$  but does not affect its relative distribution except  $E_{\hat{X}}(0)=0$ . Thus, RevIN preserves the relative spectral energy distribution and leaves the Mid-Frequency Spectrum Gap unresolved. However, our experiments still employ RevIN to ensure a fair comparison with other baselines.

Impact of High- and Low-pass filter We still define  $\hat{x}(t)$  to be the filtered (processed) signal, obtained by applying a filter H(f) (High/Low-pass filter). The filter H(f) is 1 in the passband (High/Low frequency) and 0 in the stopband (Middle frequency). So  $E_{\hat{X}}(f) = 0$ ,  $E_{\hat{X}} \leq E_X(f)$  for middle frequencies, which creates even larger gap.

#### 3.3 Overall Structure of The Proposed ReFocus

In this section, we elucidate the overall architecture of **ReFocus**, depicted in Figure 2. We define frequency domain projection as  $D1 \to D2$  representing a projection from dimension D1 to D2 in the frequency domain (Xu et al., 2024b). Initially, we apply **AMEO** to the input  $X \in \mathbb{R}^{C \times T}$ , yielding the processed spectrum  $X_{am} \in \mathbb{R}^{C \times T}$ . Next, we use a projection  $T \to D$  to transform  $X_{am}$  into the Variate Embedding  $X_{em} \in \mathbb{R}^{C \times D}$  (Liu et al., 2024b). Then,  $X_{em}$  go through N **EKPB** to generate representation  $H_{N+1}$ , which is projected to obtain final prediction  $\hat{Y}$ .

**Adaptive Mid-Frequency Energy Optimizer** Building upon the **Preliminary Analysis**, we propose a convolution- and residual learning-based solution to address the Mid-Frequency Spectrum Gap, which we denoted as AMEO.

**Definition 3.4** (Adaptive Mid-Frequency Energy Optimizer). AMEO is defined as:

$$\hat{x}(t) = x(t) - \frac{\beta}{K} \sum_{k=0}^{K-1} \tilde{x}(t+K-1-k),$$

$$\tilde{x}(t) = \begin{cases} x(t-(\frac{K}{2}+1)), & \text{if } \frac{K}{2}+1 \le t < T+\frac{K}{2}+1, \\ 0, & \text{if } 0 \le t < \frac{K}{2}+1 \text{ or } T+\frac{K}{2}+1 \le t < T+K. \end{cases}$$
(4)

It is equivalent to  $x = x - \beta \cdot Conv(x)$ . Conv is a 1D convolution (Zero-padding at both ends, stride s = 1, kernel size K, with values initialized as  $\frac{1}{K}$ ).  $\beta \in \mathbb{R}^1$  is a hyperparameter.

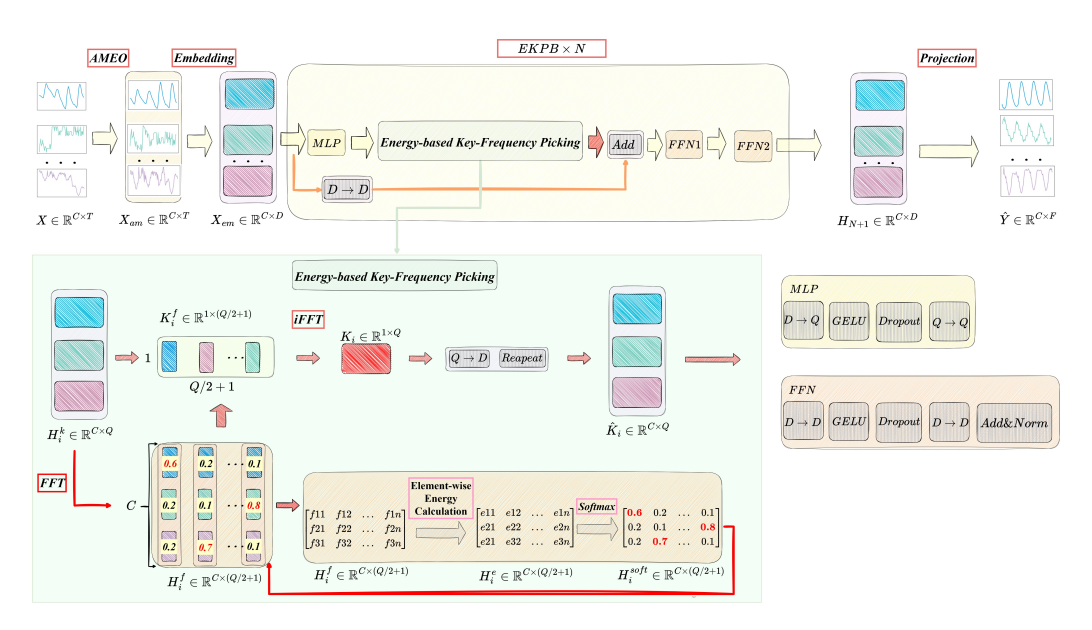


Figure 2: General structure of **ReFocus**. 'Adaptive Mid-Frequency Energy Optimizer (AMEO)' enhances mid-frequency components modeling, and 'Energy-based Key-Frequency Picking Block' (EKPB) effectively captures shared Key-Frequency across channels

**Theorem 3.5** (Frequency Spectrum after AMEO). The spectral energy of  $\hat{x}(t)$  obtained using AMEO:

$$E_{\hat{X}}(f) = |X(f)|^2 \left\{ 1 - \beta \cdot \underbrace{\frac{1}{K} \sum_{k=0}^{K-1} e^{i2\pi f(\frac{K}{2} - k - 2)/T - 1}}_{G(f)} \right\}^2$$
 (5)

The proof is in Appendix A.2. We have  $E_{\hat{X}}(f) = |X(f)|^2 (1 - \beta \cdot G(f))^2$ . Generally, G(f) behaves as a decay function, gradually reducing its value from **One** to **Zero**. Such **decay behavior** makes AMEO relatively enhances mid-frequency components, thus addressing the Mid-Frequency Spectrum Gap.

Energy-based Key-Frequency Picking Block In each EKPB, the input  $H_i \in \mathbb{R}^{C \times D}(H_1 = X_{em})$  is first processed through an MLP to generate  $H_i^k \in \mathbb{R}^{C \times Q}$ . Then, FFT is applied to get  $H_i^f \in \mathbb{R}^{C \times (Q/2+1)}$ . For  $H_i^f$ , we calculate its energy, denoted as  $H_i^e \in \mathbb{R}^{C \times (Q/2+1)}$ . A cross-channel softmax is then applied to  $H_i^e$  per frequency to obtain a probability distribution  $H_i^{soft} \in \mathbb{R}^{C \times (Q/2+1)}$ . Using  $H_i^{soft}$ , we select values from  $H_i^f$  across channels for each frequency, resulting in  $K_i^f \in \mathbb{R}^{1 \times (Q/2+1)}$ , which represents the Shared Key-Frequency across all channels. Then iFFT is performed on  $K_i^f$  to get  $K_i \in \mathbb{R}^{1 \times Q}$ , followed by projection  $Q \to D$  and repeating (C times) to get  $\hat{K}_i \in \mathbb{R}^{C \times D}$ . This  $\hat{K}_i$  is point-wisely added to  $\hat{H}_i \in \mathbb{R}^{C \times D}$ , which is the projection of  $H_i$  using projection  $D \to D$ . Then, an MLP and Add&Norm is applied to the result  $HK \in \mathbb{R}^{C \times D}$  to fuse inter-series dependencies information, and another MLP and Add&Norm is used to capture intra-series variations (Liu et al., 2024b). The output of each EKPB is  $\hat{O}_i \in \mathbb{R}^{C \times D}$ , where  $H_{i+1} = \hat{O}_i$ .

# 3.4 Key-Frequency Enhanced Training strategy

In real-world time series, certain channels often exhibit spectral dependencies, which may not be fully captured in the training set, and the specific channels with such dependencies are also unknown (Geweke, 1984; Zhao & Shen, 2024). So this work borrows insight from recent advancement of mix-up in time series (Zhou et al., 2023; Ansari et al., 2024), randomly introducing spectral

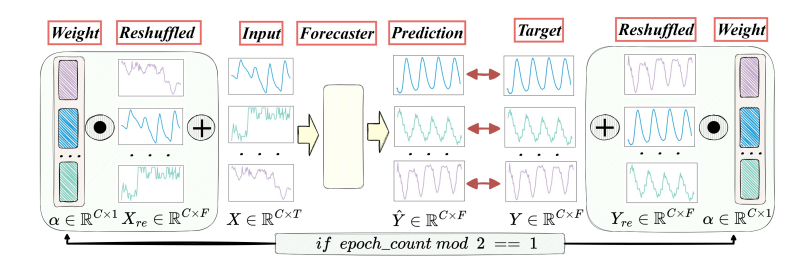


Figure 3: General process of the **Key-Frequency Enhanced Training strategy (KET)**, where spectral information from other channels is randomly introduced into each channel, to enhance the extraction of the shared Key-Frequency.

information from other channels into each channel, to enhance the extraction of the shared Key-Frequency, as in Figure 3. Given a multivariate time series input  $X \in \mathbb{R}^{C \times T}$  and its ground-truth  $Y \in \mathbb{R}^{C \times F}$ , we generate a pseudo sample pair:

$$X' = iFFT(FFT(X) + \alpha \cdot FFT(X[perm, :])),$$
  

$$Y' = iFFT(FFT(Y) + \alpha \cdot FFT(Y[perm, :])).$$
 (6)

 $\alpha \in \mathbb{R}^{C \times 1}$  is a weight vector sampled from a normal distribution, perm is a reshuffled channel index. Since FFT and iFFT are linear operations, this mix-up process can be equivalently simplified in the **Time Domain**:

$$X' = X + \alpha \cdot X[\text{perm},:],$$
  

$$Y' = Y + \alpha \cdot Y[\text{perm},:]$$
(7)

We alternate training between real and synthetic data to preserve the spectral dependencies in real samples. This combines the advantages of data augmentation, such as improved generalization, while mitigating potential drawbacks like over-smoothing and training instability (Ryu et al., 2024; Alkhalifah et al., 2022).

## 4 EXPERIMENTS

#### 4.1 EXPERIMENTAL SETTINGS

This section first introduces the whole experiment settings under a fair comparison. Secondly, we illustrate the experiment results by comparing **ReFocus** with the **TEN** well-acknowledged baselines. Further, we conducted an ablation study to comprehensively investigate the effectiveness of the 'Adaptive Mid-Frequency Energy Optimizer' (**AMEO**), 'Energy-based Key-Frequency Picking Block' (**EKPB**), and 'Key-Frequency Enhanced Training strategy' (**KET**).

**Datasets** We conduct extensive experiments on selected **Eight** widely-used real-world multivariate time series forecasting datasets, including Electricity Transformer Temperature (ETTh1, ETTh2, ETTm1, and ETTm2) (Zhou et al., 2022a), Electricity, Traffic, Weather used by Autoformer (Wu et al., 2021), and Solar\_Energy datasets proposed in LSTNet (Lai et al., 2018). For a fair comparison, we follow the same standard protocol (Liu et al., 2024b) and split all forecasting datasets into training, validation, and test sets by the ratio of 6:2:2 for the ETT dataset and 7:1:2 for the other datasets. More can be found in the Appendix.

**Evaluation protocol** Following TimesNet (Wu et al., 2023), we use Mean Squared Error (MSE) and Mean Absolute Error (MAE) for the evaluation. We follow the same evaluation protocol, where the input length is set as T=96 and the forecasting lengths  $F\in\{96,192,336,720\}$ . All the experiments are conducted on a single NVIDIA GeForce RTX 4090 with 24G VRAM. The MSE loss function is utilized for model optimization. To foster reproducibility, we make our code, and training scripts available in this **Anonymous Repo**<sup>1</sup>. Full implementation details are in Appendix B.

<sup>1</sup>https://anonymous.4open.science/r/ReFocus-2889

Baseline setting We carefully choose TEN well-acknowledged forecasting models as our baselines, including 1) Transformer-based methods: iTransformer (Liu et al., 2024b), Crossformer (Zhang & Yan, 2023), PatchTST (Nie et al., 2023); 2) Linear-based methods: TSMixer (Chen et al., 2023), DLinear (Zeng et al., 2023); 3) TCN-based methods: TimesNet (Wu et al., 2023), ModernTCN (Donghao & Xue, 2024); 4)Recent cutting-edge frequency-based methods that discussed earlier: FilterNet (Yi et al., 2024), FITS (Xu et al., 2024b), FreTS (Yi et al., 2023c). These models represent the latest advancements in multivariate time series forecasting and encompass all mainstream prediction model types. The results of ModernTCN, FilterNet, FITS, and FreTS are taken from FilterNet (Yi et al., 2024) and other results are taken from iTransformer (Liu et al., 2024b).

#### 4.2 EXPERIMENT RESULTS

Table 1: Multivariate forecasting results with prediction lengths  $F \in \{96, 192, 336, 720\}$  and fixed lookback length T = 96. Results are averaged from all prediction lengths. The best is **Red** and the second is **Blue**. The **Lower MSE/MAE** indicates the better prediction result. Full results are in Appendix K.1.

Models	ReFocus (Ours)	FilterNet (2024)	iTransf (202			rnTCN 024)		TS 24b)	Patcl (20	nTST 23)		former 023)	Time (20	esNet (23)	TSM (20		DLinea (2023)		Fre' (202	
Metric	MSE MAE	MSE MAI	E MSE	MAE	MSE	MAE	MSE	MAE	MSE	MAE	MSE	MAE	MSE	MAE	MSE	MAE	MSE M	AE   I	MSE :	MAE
ETTm1	0.387 0.394	0.392 0.40	1   0.407	0.410	0.389	0.402	0.415	0.408	0.387	0.400	0.513	0.496	0.400	0.406	0.398	0.407	0.403 0.4	107   0	0.408	0.416
ETTm2	0.275 0.320	0.285 0.32	8   0.288	0.332	0.279	0.322	0.286	0.328	0.281	0.326	0.757	0.610	0.291	0.333	0.289	0.333	0.350 0.4	101   0	0.321	0.368
ETTh1	0.434 0.433	0.441 0.43	0.454	0.447	0.446	0.433	0.451	0.440	0.469	0.454	0.529	0.522	0.458	0.450	0.463	0.452	0.456 0.4	152   0	).475	0.463
ETTh2	0.371 0.396	0.383 0.40	7   0.383	0.407	0.382	<u>0.404</u>	0.383	0.408	0.387	0.407	0.942	0.684	0.414	0.427	0.401	0.417	0.559 0.5	515   0	0.472	0.465
ECL	0.168 0.262	0.173 0.26	0.178	0.270	0.197	0.282	0.217	0.295	0.205	0.290	0.244	0.334	0.192	0.295	0.186	0.287	0.212 0.3	800   0	0.189	0.278
Traffic	0.412 0.265	0.463 0.31	0   0.428	0.282	0.546	0.348	0.627	0.376	0.481	0.304	0.550	0.304	0.620	0.336	0.522	0.357	0.625 0.3	883   0	0.618	0.390
Weather	0.245 0.271	0.245 0.27	0.258	0.279	0.247	0.272	0.249	0.276	0.259	0.281	0.259	0.315	0.259	0.287	0.256	0.279	0.265 0.3	317	0.250	0.270
Solar_Energy	0.222 0.252	0.243 0.28	1 0.233	0.262	0.244	0.286	0.395	0.407	0.270	0.307	0.641	0.639	0.301	0.319	0.260	0.297	0.330 0.4	101   0	0.248	0.296

Quantitative comparison Comprehensive forecasting results are listed in Table 1. We leave full forecasting results in APPENDIX to save place. It is quite evident that **ReFocus** has demonstrated superior predictive performance across all datasets, significantly outperforming the second-best method. Especially, Compared to the previous SOTA **iTransformer**, we have reduced the MSE by **4%**, **6%**, and **5%** on the three most challenging benchmarks: Traffic, ECL, and Solar, respectively, indicating a significant breakthrough. These significant improvements indicate that the **ReFocus** model possesses robust performance and broad applicability in multivariate time series forecasting tasks, especially in tasks with a large number of channels, such as the Solar\_Energy dataset (**137** channels), ECL dataset (**321** channels), and Traffic dataset (**862** channels).

#### 4.3 MODEL ANALYSIS

Table 2: Ablation of 'Adaptive Mid-Frequency Energy Optimizer (AMEO)' and 'Key-Frequency Enhanced Training strategy (KET)'. We list the average results. Full results are in Appendix K.2.

AMEO	KET	ET	Γm1	ET.	Γm2	ET	Γh1	ET	Γh2	Е	CL	Tra	ffic	Wea	ther	Solar_	Energy
		MSE	MAE	MSE	MAE												
-	-	0.401	0.403	0.283	0.325	0.440	0.437	0.376	0.400	0.178	0.270	0.449	0.289	0.252	0.278	0.232	0.264
-																	0.258
$\checkmark$	-	0.393	0.402	0.282	0.326	0.443	0.440	0.372	0.397	0.174	0.267	0.452	0.289	0.248	0.275	0.231	0.261
$\checkmark$	<b>√</b>	0.387	0.394	0.275	0.320	0.434	0.433	0.371	0.396	0.168	0.262	0.412	0.265	0.245	0.271	0.222	0.252

**Ablation study of AMEO and KET** To evaluate the contributions of each module in ReFocus, we performed ablation studies on the 'Adaptive Mid-Frequency Energy Optimizer (AMEO)' and the 'Key-Frequency Enhanced Training (KET)' strategy. The results are summarized in Table 2. Notably, integrating both modules achieves the best performance, highlighting the effectiveness of their synergy. Additionally, each module delivers substantial improvements over baseline models in most cases.

**Further study of KET** We conducted further ablation studies on the KET to demonstrate the importance of alternate training between real and synthetic data. The experimental results in

Table 3: Further ablation of 'Key-Frequency Enhanced Training strategy (**KET**)'. 'Real' means KET is not performed, i.e. trained on original data. 'Pseudo' means trained on Pseudo samples. If both are used (Bottom Line), this means the model is trained on Real and Pseudo samples alternatively, i.e. **KET**. We list the average results. Full results are in Appendix K.3.

Real	Pseudo	ET	Γm1	ET	Γm2	ET	Th1	ET	Th2	Е	CL	Tra	iffic	Wea	ather	Solar_	Energy
		MSE	MAE	MSE	MAE												
<b>√</b>	-	0.401	0.403	0.283	0.325	0.440	0.437	0.376	0.400	0.178	0.270	0.449	0.289	0.252	0.278	0.232	0.264
-	✓	0.396	0.398	0.280	0.323	0.436	0.434	0.372	0.397	0.175	0.266	0.417	0.271	0.252	0.276	0.277	0.294
$\checkmark$	✓	0.394	0.396	0.279	0.322	0.437	0.435	0.373	0.398	0.171	0.263	0.414	0.268	0.250	0.275	0.228	0.258

Table 3 reveal that while training on pseudo samples can partially enhance the model's generalization performance on the test set, it also tends to cause over-smoothing and training instability on more complex datasets, such as Solar\_Energy. In contrast, training on real and synthetic data alternatively (KET) improves generalization and mitigates over-smoothing and training instability by preserving the spectral dependencies of real samples. More Analyses are in Appendix C.

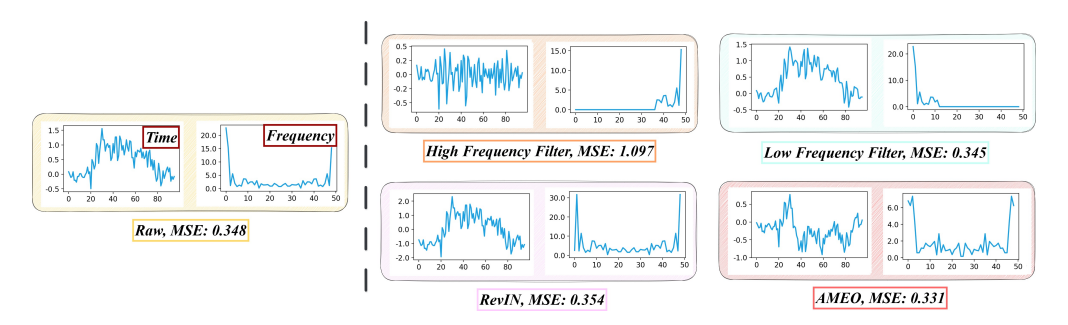


Figure 4: The time-frequency domain visualization of the original sequence (ETTm1, *the last variate*), the sequence processed by high-pass and low-pass filters, by RevIN, and by AMEO. We selected the input-96-forecast-96 task.

Superiority of AMEO over RevIN and Filters We investigated the roles of AMEO, RevIN, and Filters in addressing the Mid-Frequency Spectrum Gap through time-frequency domain visualization analysis. The results presented in Figure 4 align perfectly with our previous theoretical analysis. High-pass and low-pass filters fail to address the Mid-Frequency Spectrum Gap and exacerbate this issue. RevIN, on the other hand, merely eliminates the energy of the zero-frequency component while scaling other components using the variance  $\sigma^2$ , which also does not effectively resolve the problem. In contrast, our AMEO successfully amplifies the mid-frequency energy. Furthermore, compared to the original sequence and the sequence processed by RevIN, we observe that the sequence processed by AMEO exhibits significantly higher stationarity with much more stable means and variance. More Analyses are in Appendix F.

Outstanding inter-series modeling ability of the EKPB In the multivariate correlation analysis in Figure 5 (LEFT), the early encoder layer produces correlation maps similar to the input series X. In deeper layers, these maps gradually resemble the correlation patterns of the target series Y, suggesting that ReFocus effectively models inter-series dependencies in a hierarchical and progressive manner. Furthermore, Figure 5 (RIGHT) indicates that ReFocus effectively captures Key-Frequency shared across channels. To illustrate EKPB's functionality, we visualize the series embeddings with and without its adjustment in Figure 6 (LEFT). The T-SNE visualization of the series embeddings shows that without EKPB, using only the channel-independent strategy (Nie et al., 2023), the MSE is 0.171. After applying EKPB, channels sharing Key-Frequency (variates 2&3) are clustered, while others (variates 1&3) are separated. This adjustment improves the MSE from 0.171 to 0.145, a 15% reduction.

#### **Efficiency Analysis of ReFocus**

ReFocus delivers higher performance with minimal memory and time consumption. We left the detailed complexity analysis and more information in Appendix H, which shows that our ReFcous with only **Linear** complexity. It achieves better performance with significantly lower resource

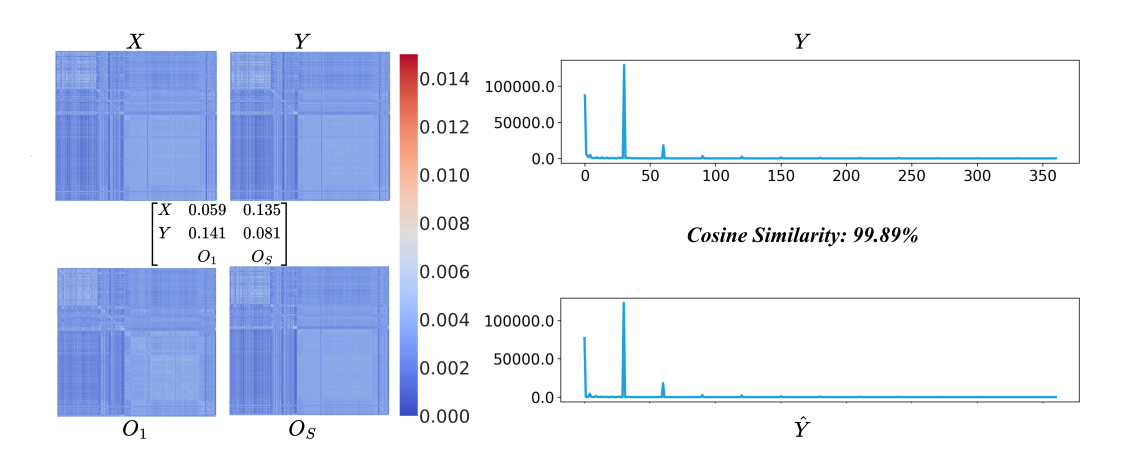


Figure 5: Analysis of multivariate correlation (Left) and Shared Key-Frequency (Right) on ECL, with *input-96-forecast-720*. **Left**: Visualization of multivariate correlations of raw time series (X, Y) and the learned embedding  $(O_1, O_S)$ .  $O_1$  is the output embedding of the first encoder block, and  $O_S$  the last block. Frobenius norm  $\|A - B\|_F = \sqrt{\sum_{i,j} (A_{ij} - B_{ij})^2}$  is used to quantify the similarity (shown in Figure center). The lower, the higher. More examples and details are in Appendix G. **Right**: We visualize the average spectral energy across all channels for both the ground truth samples Y and the predictions  $\hat{Y}$ .

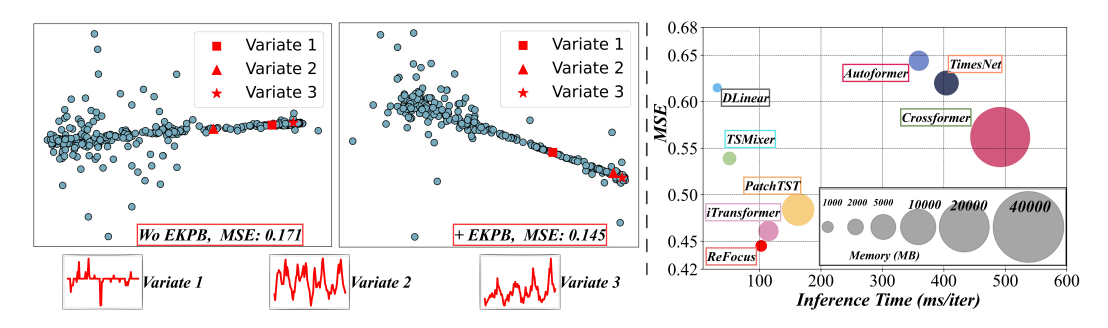


Figure 6: Left: T-SNE visualization of the series embeddings with and without 'Energy-based Key-Frequency Picking Block' (EKPB) on ECL. We choose the input-96-forecast-96 task. Three example variates are highlighted: variates 2&3 shared a common Key-Frequency, while variate 1 does not. Right: Memory and time consumption of different models. CoIn-based models demonstrate efficient performance with minimal memory and computational overhead.

consumption, as in Figure 6 (**RIGHT**). ReFocus remains competitive even against other Linear-based or MLP-based approaches, such as DLinear and TSMixer.

#### 5 CONCLUSION

This work addresses two critical challenges in multivariate time series forecasting: the Mid-Frequency Spectrum Gap and the efficient modeling of the shared Key-Frequency. We propose the 'Adaptive Mid-Frequency Energy Optimizer', which effectively enhances mid-frequency extraction, and the 'Energy-based Key-Frequency Picking Block' with the 'Key-Frequency Enhanced Training' strategy, which efficiently captures shared frequency patterns. Extensive experiments demonstrate the superiority of our approach, achieving up to 6% MSE reduction on challenging benchmarks, thus advancing the SOTA in frequency-domain forecasting.

# REFERENCES

- Md Atik Ahamed and Qiang Cheng. Timemachine: A time series is worth 4 mambas for long-term forecasting. arXiv preprint arXiv:2403.09898, 2024. URL https://arxiv.org/abs/2403.09898.
- Tariq Alkhalifah, Hui Wang, and Oleg Ovcharenko. Mlreal: Bridging the gap between training on synthetic data and real data applications in machine learning. *Artificial Intelligence in Geosciences*, 3:101–114, 2022.
- Davide Anguita, Alessandro Ghio, Luca Oneto, Xavier Parra, Jorge Luis Reyes-Ortiz, et al. A public domain dataset for human activity recognition using smartphones. In *Esann*, volume 3, pp. 3–4, 2013.
- Abdul Fatir Ansari, Lorenzo Stella, Caner Turkmen, Xiyuan Zhang, Pedro Mercado, Huibin Shen, Oleksandr Shchur, Syama Sundar Rangapuram, Sebastian Pineda Arango, Shubham Kapoor, et al. Chronos: Learning the language of time series. *arXiv preprint arXiv:2403.07815*, 2024.
- Richard Asselin. Frequency filter for time integrations. *Monthly Weather Review*, 100(6):487–490, 1972.
- Shaojie Bai, J Zico Kolter, and Vladlen Koltun. An empirical evaluation of generic convolutional and recurrent networks for sequence modeling. *arXiv preprint arXiv:1803.01271*, 2018.
- Juan Bógalo, Pilar Poncela, and Eva Senra. Understanding fluctuations through multivariate circulant singular spectrum analysis. *Expert Systems with Applications*, 251:123827, 2024.
- Yigit Baran Can and Radu Timofte. An efficient cnn for spectral reconstruction from rgb images. *arXiv preprint arXiv:1804.04647*, 2018.
- Tanmay Chakraborty and Utkarsh Trehan. Spectralnet: Exploring spatial-spectral waveletcnn for hyperspectral image classification. *arXiv preprint arXiv:2104.00341*, 2021.
- Chris Chatfield and Haipeng Xing. *The analysis of time series: an introduction with R*. Chapman and hall/CRC, 2019.
- Mickaël D Chekroun and Dmitri Kondrashov. Data-adaptive harmonic spectra and multilayer stuart-landau models. *Chaos: An Interdisciplinary Journal of Nonlinear Science*, 27(9), 2017.
- Jialin Chen, Jan Eric Lenssen, Aosong Feng, Weihua Hu, Matthias Fey, Leandros Tassiulas, Jure Leskovec, and Rex Ying. From similarity to superiority: Channel clustering for time series forecasting. *arXiv preprint arXiv:2404.01340*, 2024. URL https://arxiv.org/abs/2404.01340.
- Si-An Chen, Chun-Liang Li, Sercan O Arik, Nathanael Christian Yoder, and Tomas Pfister. Tsmixer: An all-mlp architecture for time series forecasting. *Transactions on Machine Learning Research*, 2023. ISSN 2835-8856. URL https://openreview.net/forum?id=wbpxTuXgm0.
- Changqing Cheng, Akkarapol Sa-Ngasoongsong, Omer Beyca, Trung Le, Hui Yang, Zhenyu Kong, and Satish TS Bukkapatnam. Time series forecasting for nonlinear and non-stationary processes: a review and comparative study. *Iie Transactions*, 47(10):1053–1071, 2015.
- Razvan-Gabriel Cirstea, Chenjuan Guo, Bin Yang, Tung Kieu, Xuanyi Dong, and Shirui Pan. Triformer: Triangular, variable-specific attentions for long sequence multivariate time series forecasting–full version. *arXiv preprint arXiv:2204.13767*, 2022.
- Tao Dai, Beiliang Wu, Peiyuan Liu, Naiqi Li, Jigang Bao, Yong Jiang, and Shu-Tao Xia. Periodicity decoupling framework for long-term series forecasting. In *The Twelfth International Conference on Learning Representations*, 2024.
- Abhimanyu Das, Weihao Kong, Andrew Leach, Shaan K Mathur, Rajat Sen, and Rose Yu. Long-term forecasting with tide: Time-series dense encoder. *Transactions on Machine Learning Research*, 2023. ISSN 2835-8856. URL https://openreview.net/forum?id=pCbC3aQB5W.

- Jiaxiang Dong, Haixu Wu, Haoran Zhang, Li Zhang, Jianmin Wang, and Mingsheng Long.
  Simmtm: A simple pre-training framework for masked time-series modeling. In *Proceedings of the Thirty-seventh Conference on Neural Information Processing Systems*, 2023. URL https://openreview.net/forum?id=ginTcBUnL8.
  - Luo Donghao and Wang Xue. Modernton: A modern pure convolution structure for general time series analysis. In *Proceedings of the Twelfth International Conference on Learning Representations*, 2024. URL https://openreview.net/forum?id=vpJMJerXHU.
  - Dazhao Du, Bing Su, and Zhewei Wei. Preformer: Predictive transformer with multi-scale segment-wise correlations for long-term time series forecasting. In *ICASSP 2023-2023 IEEE International Conference on Acoustics, Speech and Signal Processing (ICASSP)*. IEEE, 2023.
  - Emadeldeen Eldele, Mohamed Ragab, Zhenghua Chen, Min Wu, and Xiaoli Li. Tslanet: Rethinking transformers for time series representation learning. In *International Conference on Machine Learning*, 2024.
  - Wei Fan, Kun Yi, Hangting Ye, Zhiyuan Ning, Qi Zhang, and Ning An. Deep frequency derivative learning for non-stationary time series forecasting. *arXiv preprint arXiv:2407.00502*, 2024.
  - John F Geweke. Measures of conditional linear dependence and feedback between time series. *Journal of the American Statistical Association*, 79(388):907–915, 1984.
  - Clive WJ Granger and Paul Newbold. Spurious regressions in econometrics. *Journal of econometrics*, 2(2):111–120, 1974.
  - Hongyu Guo, Yongyi Mao, and Richong Zhang. Mixup as locally linear out-of-manifold regularization. In *Proceedings of the AAAI conference on artificial intelligence*, volume 33, pp. 3714–3722, 2019.
  - Lu Han, Xu-Yang Chen, Han-Jia Ye, and De-Chuan Zhan. Softs: Efficient multivariate time series forecasting with series-core fusion. *arXiv preprint arXiv:2404.14197*, 2024. URL https://arxiv.org/abs/2404.14197.
  - Maowei Jiang, Pengyu Zeng, Kai Wang, Huan Liu, Wenbo Chen, and Haoran Liu. Fecam: Frequency enhanced channel attention mechanism for time series forecasting. *Advanced Engineering Informatics*, 58:102158, 2023.
  - Ming Jin, Shiyu Wang, Lintao Ma, Zhixuan Chu, James Y. Zhang, Xiaoming Shi, Pin-Yu Chen, Yuxuan Liang, Yuan-Fang Li, Shirui Pan, and Qingsong Wen. Time-LLM: Time series forecasting by reprogramming large language models. In *Proceedings of the Twelfth International Conference on Learning Representations (ICLR)*, 2024. URL https://openreview.net/forum?id=Unb5CVPtae.
  - Taesung Kim, Jinhee Kim, Yunwon Tae, Cheonbok Park, Jang-Ho Choi, and Jaegul Choo. Reversible instance normalization for accurate time-series forecasting against distribution shift. In *International Conference on Learning Representations*, 2022. URL https://openreview.net/forum?id=cGDAkQolCOp.
  - Guokun Lai, Wei-Cheng Chang, Yiming Yang, and Hanxiao Liu. Modeling long-and short-term temporal patterns with deep neural networks. In *Proceedings of the 41st International ACM SIGIR Conference on Research & Development in Information Retrieval*, pp. 95–104, 2018.
  - Oscar D Lara and Miguel A Labrador. A survey on human activity recognition using wearable sensors. *IEEE communications surveys & tutorials*, 15(3):1192–1209, 2012.
  - Zhe Li, Shiyi Qi, Yiduo Li, and Zenglin Xu. Revisiting long-term time series forecasting: An investigation on linear mapping. *arXiv preprint arXiv:2305.10721*, 2023.
- Bryan Lim and Stefan Zohren. Time series forecasting with deep learning: A survey. *Philosophical Transactions of the Royal Society A: Mathematical, Physical and Engineering Sciences*, pp. 20200209, 2021. doi: 10.1098/rsta.2020.0209. URL http://dx.doi.org/10.1098/rsta.2020.0209.

- Shengsheng Lin, Weiwei Lin, Wentai Wu, Feiyu Zhao, Ruichao Mo, and Haotong Zhang. Segrnn: Segment recurrent neural network for long-term time series forecasting. *arXiv* preprint *arXiv*:2308.11200, 2023. URL https://arxiv.org/abs/2308.11200.
  - Juncheng Liu, Chenghao Liu, Gerald Woo, Yiwei Wang, Bryan Hooi, Caiming Xiong, and Doyen Sahoo. Unitst: Effectively modeling inter-series and intra-series dependencies for multivariate time series forecasting. *arXiv* preprint arXiv:2406.04975, 2024a. URL https://arxiv.org/abs/2406.04975.
  - Minhao Liu, Ailing Zeng, Muxi Chen, Zhijian Xu, Qiuxia Lai, Lingna Ma, and Qiang Xu. Scinet: Time series modeling and forecasting with sample convolution and interaction. In Alice H. Oh, Alekh Agarwal, Danielle Belgrave, and Kyunghyun Cho (eds.), *Advances in Neural Information Processing Systems*, 2022a. URL https://openreview.net/forum?id=AyajSjTAzmq.
  - Shizhan Liu, Hang Yu, Cong Liao, Jianguo Li, Weiyao Lin, Alex X. Liu, and Schahram Dustdar. Pyraformer: Low-complexity pyramidal attention for long-range time series modeling and forecasting. In *International Conference on Learning Representations*, 2022b. URL https://openreview.net/forum?id=0EXmFzUn5I.
  - Yong Liu, Haixu Wu, Jianmin Wang, and Mingsheng Long. Non-stationary transformers: Exploring the stationarity in time series forecasting. In *Advances in Neural Information Processing Systems*, 2022c. URL https://openreview.net/forum?id=ucNDIDRNjjv.
  - Yong Liu, Tengge Hu, Haoran Zhang, Haixu Wu, Shiyu Wang, and Mingsheng Long. itransformer: Inverted transformers are effective for time series forecasting. In *Proceedings of the Twelfth International Conference on Learning Representations*, 2024b. URL https://openreview.net/forum?id=JePfAI8fah.
  - Yong Liu, Guo Qin, Xiangdong Huang, Jianmin Wang, and Mingsheng Long. Autotimes: Autoregressive time series forecasters via large language models. *arXiv preprint arXiv:2402.02370*, 2024c.
  - Yong Liu, Guo Qin, Xiangdong Huang, Jianmin Wang, and Mingsheng Long. Autotimes: Autoregressive time series forecasters via large language models. *arXiv preprint arXiv:2402.02370*, 2024d.
  - William T Ng, K Siu, Albert C Cheung, and Michael K Ng. Expressing multivariate time series as graphs with time series attention transformer. *arXiv preprint arXiv:2208.09300*, 2022. URL https://arxiv.org/abs/2208.09300.
  - Yuqi Nie, Nam H Nguyen, Phanwadee Sinthong, and Jayant Kalagnanam. A time series is worth 64 words: Long-term forecasting with transformers. In *Proceedings of the Eleventh International Conference on Learning Representations*, 2023. URL https://openreview.net/forum?id=Jbdc0vTOcol.
  - Ernst Niedermeyer and FH Lopes da Silva. *Electroencephalography: basic principles, clinical applications, and related fields.* Lippincott Williams & Wilkins, 2005.
  - Boris N. Oreshkin, Dmitri Carpov, Nicolas Chapados, and Yoshua Bengio. N-beats: Neural basis expansion analysis for interpretable time series forecasting. In *International Conference on Learning Representations*, 2020. URL https://openreview.net/forum?id=rlecqn4YwB.
  - Daniel S Park, William Chan, Yu Zhang, Chung-Cheng Chiu, Barret Zoph, Ekin D Cubuk, and Quoc V Le. Specaugment: A simple data augmentation method for automatic speech recognition. *arXiv* preprint arXiv:1904.08779, 2019.
  - Xihao Piao, Zheng Chen, Taichi Murayama, Yasuko Matsubara, and Yasushi Sakurai. Fredformer: Frequency debiased transformer for time series forecasting. In *Proceedings of the 30th ACM SIGKDD Conference on Knowledge Discovery and Data Mining*, KDD '24, 2024.
  - Nasim Rahaman, Aristide Baratin, Devansh Arpit, Felix Draxler, Min Lin, Fred Hamprecht, Yoshua Bengio, and Aaron Courville. On the spectral bias of neural networks. In *International conference on machine learning*, pp. 5301–5310. PMLR, 2019.

- Hyun Ryu, Sunjae Yoon, Hee Suk Yoon, Eunseop Yoon, and Chang D Yoo. Simpsi: A simple strategy to preserve spectral information in time series data augmentation. In *Proceedings of the AAAI Conference on Artificial Intelligence*, volume 38, pp. 14857–14865, 2024.
  - Zongjiang Shang, Ling Chen, Binqing Wu, and Dongliang Cui. Ada-mshyper: Adaptive multi-scale hypergraph transformer for time series forecasting. In *The Thirty-eighth Annual Conference on Neural Information Processing Systems*, 2024.
  - James H Stock and Mark W Watson. Forecasting using principal components from a large number of predictors. *Journal of the American statistical association*, 97(460):1167–1179, 2002.
  - Raanju R Sundararajan and Scott A Bruce. Frequency band analysis of nonstationary multivariate time series. *arXiv preprint arXiv:2301.03664*, 2023.
  - Naftali Tishby and Noga Zaslavsky. Deep learning and the information bottleneck principle. In 2015 IEEE Information Theory Workshop (ITW), Apr 2015. doi: 10.1109/itw.2015.7133169. URL http://dx.doi.org/10.1109/itw.2015.7133169.
  - William Toner and Luke Nicholas Darlow. An analysis of linear time series forecasting models. In *Proceedings of the Forty-first International Conference on Machine Learning (ICML)*, 2024. URL https://openreview.net/forum?id=x182CcbYaT.
  - José F Torres, Dalil Hadjout, Abderrazak Sebaa, Francisco Martínez-Álvarez, and Alicia Troncoso. Deep learning for time series forecasting: a survey. *Big Data*, 9(1):3–21, 2021.
  - Huiqiang Wang, Jian Peng, Feihu Huang, Jince Wang, Junhui Chen, and Yifei Xiao. MICN: Multi-scale local and global context modeling for long-term series forecasting. In *The Eleventh International Conference on Learning Representations*, 2023. URL https://openreview.net/forum?id=zt53IDUR1U.
  - Shiyu Wang, Haixu Wu, Xiaoming Shi, Tengge Hu, Huakun Luo, Lintao Ma, James Y Zhang, and JUN ZHOU. Timemixer: Decomposable multiscale mixing for time series forecasting. In *International Conference on Learning Representations (ICLR)*, 2024a.
  - Xue Wang, Tian Zhou, Qingsong Wen, Jinyang Gao, Bolin Ding, and Rong Jin. CARD: Channel aligned robust blend transformer for time series forecasting. In *The Twelfth International Conference on Learning Representations*, 2024b. URL https://openreview.net/forum?id=MJksrOhurE.
  - Yihe Wang, Nan Huang, Taida Li, Yujun Yan, and Xiang Zhang. Medformer: A multi-granularity patching transformer for medical time-series classification. *Advances in Neural Information Processing Systems*, 37:36314–36341, 2024c.
  - Yuxuan Wang, Haixu Wu, Jiaxiang Dong, Yong Liu, Mingsheng Long, and Jianmin Wang. Deep time series models: A comprehensive survey and benchmark. *arXiv preprint arXiv:2407.13278*, 2024d. URL https://arxiv.org/abs/2407.13278.
  - Zihan Wang, Fanheng Kong, Shi Feng, Ming Wang, Han Zhao, Daling Wang, and Yifei Zhang. Is mamba effective for time series forecasting? *arXiv* preprint arXiv:2403.11144, 2024e.
  - Qingsong Wen, Tian Zhou, Chaoli Zhang, Weiqi Chen, Ziqing Ma, Junchi Yan, and Liang Sun. Transformers in time series: A survey. *arXiv preprint arXiv:2202.07125*, 2022.
  - Haixu Wu, Jiehui Xu, Jianmin Wang, and Mingsheng Long. Autoformer: Decomposition transformers with auto-correlation for long-term series forecasting. In M. Ranzato, A. Beygelzimer, Y. Dauphin, P.S. Liang, and J. Wortman Vaughan (eds.), *Advances in Neural Information Processing Systems*, volume 34, pp. 22419–22430. Curran Associates, Inc., 2021. URL https://proceedings.neurips.cc/paper\_files/paper/2021/file/bcc0d400288793e8bdcd7c19a8ac0c2b-Paper.pdf.
  - Haixu Wu, Tengge Hu, Yong Liu, Hang Zhou, Jianmin Wang, and Mingsheng Long. TimesNet: Temporal 2d-variation modeling for general time series analysis. In *The Eleventh International Conference on Learning Representations*, 2023. URL https://openreview.net/forum?id=ju\_Uqw3840q.

704

705

706

707 708

709

710

711

712

713

714

715

716

717

718

719 720

721

722

723

724

725

726

727

728 729

730

731

732

733 734

735

736

737

738

739

740

741

742

743

744 745

746

747

748

749

750

751

752 753

754

- Zhi-Qin John Xu, Yaoyu Zhang, and Tao Luo. Overview frequency principle/spectral bias in deep 703 learning. Communications on Applied Mathematics and Computation, pp. 1–38, 2024a.
  - Zhijian Xu, Ailing Zeng, and Qiang Xu. Fits: Modeling time series with 10k parameters. In Proceedings of the Twelfth International Conference on Learning Representations, 2024b. URL https://openreview.net/forum?id=bWcnvZ3qMb.
  - Kun Yi, Qi Zhang, Longbing Cao, Shoujin Wang, Guodong Long, Liang Hu, Hui He, Zhendong Niu, Wei Fan, and Hui Xiong. A survey on deep learning based time series analysis with frequency transformation. arXiv preprint arXiv:2302.02173, 2023a.
  - Kun Yi, Qi Zhang, Wei Fan, Hui He, Liang Hu, Pengyang Wang, Ning An, Longbing Cao, and Zhendong Niu. FourierGNN: Rethinking multivariate time series forecasting from a pure graph perspective. In Thirty-seventh Conference on Neural Information Processing Systems, 2023b. URL https://openreview.net/forum?id=bGs1qWQ1Fx.
  - Kun Yi, Qi Zhang, Wei Fan, Shoujin Wang, Pengyang Wang, Hui He, Ning An, Defu Lian, Longbing Cao, and Zhendong Niu. Frequency-domain MLPs are more effective learners in time series forecasting. In Thirty-seventh Conference on Neural Information Processing Systems, 2023c. URL https://openreview.net/forum?id=iif9mGCTfy.
  - Kun Yi, Jingru Fei, Qi Zhang, Hui He, Shufeng Hao, Defu Lian, and Wei Fan. Filternet: Harnessing frequency filters for time series forecasting. arXiv preprint arXiv:2411.01623, 2024.
  - Chengqing Yu, Fei Wang, Zezhi Shao, Tao Sun, Lin Wu, and Yongjun Xu. Dsformer: A double sampling transformer for multivariate time series long-term prediction. In *Proceedings of the 32nd* ACM international conference on information and knowledge management, pp. 3062–3072, 2023.
  - Guoqi Yu, Yaoming Li, Xiaoyu Guo, Dayu Wang, Zirui Liu, Shujun Wang, and Tong Yang. Lino: Advancing recursive residual decomposition of linear and nonlinear patterns for robust time series forecasting. arXiv preprint arXiv:2410.17159, 2024a.
  - Guoqi Yu, Jing Zou, Xiaowei Hu, Angelica I Aviles-Rivero, Jing Qin, and Shujun Wang. Revitalizing multivariate time series forecasting: Learnable decomposition with inter-series dependencies and intra-series variations modeling. In Proceedings of the Forty-first International Conference on Machine Learning (ICML), 2024b. URL https://openreview.net/forum?id= 87CYNyCGOo.
  - Ailing Zeng, Muxi Chen, Lei Zhang, and Qiang Xu. Are transformers effective for time series forecasting? In Proceedings of the AAAI Conference on Artificial Intelligence, volume 37, pp. 11121-11128, 2023. URL https://ojs.aaai.org/index.php/AAAI/article/ view/26317/26089.
  - Tianping Zhang, Yizhuo Zhang, Wei Cao, Jiang Bian, Xiaohan Yi, Shun Zheng, and Jian Li. Less is more: Fast multivariate time series forecasting with light sampling-oriented mlp structures. arXiv preprint arXiv:2207.01186, 2022. URL https://arxiv.org/abs/2207.01186.
  - Yunhao Zhang and Junchi Yan. Crossformer: Transformer utilizing cross-dimension dependency for multivariate time series forecasting. In The Eleventh International Conference on Learning Representations, 2023. URL https://openreview.net/forum?id=vSVLM2j9eie.
  - Lifan Zhao and Yanyan Shen. Rethinking channel dependence for multivariate time series forecasting: Learning from leading indicators. In The Twelfth International Conference on Learning Representations, 2024. URL https://openreview.net/forum?id=JiTVtCUOpS.
  - Haoyi Zhou, Shanghang Zhang, Jieqi Peng, Shuai Zhang, Jianxin Li, Hui Xiong, and Wancai Zhang. Informer: Beyond efficient transformer for long sequence time-series forecasting. Proceedings of the AAAI Conference on Artificial Intelligence, 35:11106–11115, 2022a. doi: 10.1609/aaai.v35i12. 17325. URL http://dx.doi.org/10.1609/aaai.v35i12.17325.
  - Tian Zhou, Ziqing MA, xue wang, Qingsong Wen, Liang Sun, Tao Yao, Wotao Yin, and Rong Jin. Film: Frequency improved legendre memory model for long-term time series forecasting. In S. Koyejo, S. Mohamed, A. Agarwal, D. Belgrave, K. Cho, and A. Oh (eds.), Advances in Neural Information Processing Systems, volume 35, pp. 12677–12690. Curran Associates, Inc., 2022b.

Tian Zhou, Ziqing Ma, Qingsong Wen, Xue Wang, Liang Sun, and Rong Jin. Fedformer: Frequency enhanced decomposed transformer for long-term series forecasting. In *Proceedings of the 39th International Conference on Machine Learning (ICML 2022)*, 2022c.

Yun Zhou, Liwen You, Wenzhen Zhu, and Panpan Xu. Improving time series forecasting with mixup data augmentation. 2023.

# A PROOF

This section is dedicated to proving Theorem 3.3 and Theorem 3.5.

#### A.1 IMPACT OF REVIN ON FREQUENCY SPECTRUM

RevIN (Kim et al., 2022; Liu et al., 2022c) normalizes inputs using sample-wise mean and variance, then reverts scaling post-prediction to ensure consistent distributions, mitigating non-stationary effects in time series

Let the original time series be x(t) with length T. The series  $\hat{x}(t)$  that processed by RevIN is given by:

$$\hat{x}(t) = \frac{x(t) - \mu}{\sigma}, t = 0, 1, \dots, T - 1,$$

$$\mu = \frac{1}{T} \sum_{t=0}^{T-1} x(t), \quad \sigma = \sqrt{\frac{1}{T} \sum_{t=0}^{T-1} (x(t) - \mu)^2}.$$
(8)

The Fourier transform of x(t) and  $\hat{x}(t)$  are:

$$X(f) = \sum_{t=0}^{T-1} x(t)e^{-i2\pi ft/T-1}, \quad f = 0, 1, \dots, T-1,$$

$$\hat{X}(f) = \sum_{t=0}^{T-1} \left(\frac{x(t) - \mu}{\sigma}\right) e^{-i2\pi ft/T-1}$$

$$= \frac{1}{\sigma} \sum_{t=0}^{T-1} x(t)e^{-i2\pi ft/T-1} - \frac{\mu}{\sigma} \sum_{t=0}^{T-1} e^{-i2\pi ft/T-1}.$$
(9)

The spectral energy is computed as the squared magnitude of the Fourier transform. For x(t) and  $\hat{x}(t)$ , we have:

$$E_X(f) = |X(f)|^2, \quad E_{\hat{X}}(f) = |\hat{X}(f)|^2.$$
 (10)

When f=0, the exponential term  $e^{-i2\pi ft/T-1}=1$ , so:

$$\hat{X}(0) = \frac{1}{\sigma} \sum_{t=0}^{T-1} x(t) - \frac{\mu T}{\sigma}$$

$$= \frac{\mu T}{\sigma} - \frac{\mu T}{\sigma}$$

$$= 0$$
(11)

Since  $\frac{\mu}{\sigma}$  is a constant, we have:

$$\frac{\mu}{\sigma} \cdot \sum_{t=0}^{T-1} e^{-i2\pi f t/T - 1} = 0, \quad f = 1, 2 \dots, T - 1,$$

$$\hat{X}(f) = \frac{1}{\sigma} \sum_{t=0}^{T-1} x(t) e^{-i2\pi f t/T - 1} - \frac{\mu}{\sigma} \sum_{t=0}^{T-1} e^{-i2\pi f t/T - 1}$$

$$= \frac{1}{\sigma} X(f),$$

$$E_{\hat{X}}(f) = \left(\frac{1}{\sigma}\right)^2 |X(f)|^2.$$
(12)

This suggests that RevIN scales the spectral energy by  $\sigma^2$  but does not affect its relative distribution except  $\hat{X}(0) = 0$ . Thus, RevIN preserves the relative spectral energy distribution and leaves the Mid-Frequency Spectrum Gap unresolved.

#### A.2 IMPACT OF AMEO ON FREQUENCY SPECTRUM

Referring back to Definition 3.4, AMEO is defined as:

$$\hat{x}(t) = x(t) - \frac{\beta}{K} \sum_{k=0}^{K-1} \tilde{x}(t+K-1-k),$$

$$\tilde{x}(t) = \begin{cases} x(t-(\frac{K}{2}+1)), & \text{if } \frac{K}{2}+1 \le t < T+\frac{K}{2}+1\\ 0, & \text{if } 0 \le t < \frac{K}{2}+1 \text{ or } T+\frac{K}{2}+1 \le t < T+K \end{cases}$$
(13)

The Fourier transform of  $\hat{x}(t)$  is:

$$\hat{X}(f) = \sum_{t=0}^{T-1} \left[ x(t) - \frac{\beta}{K} \sum_{k=0}^{K-1} \tilde{x}(t+K-1-k) \right] e^{-i2\pi f t/T - 1}$$

$$= \underbrace{\sum_{t=0}^{T-1} x(t) e^{-i2\pi f t/T - 1}}_{X(f)} - \frac{\beta}{K} \sum_{k=0}^{K-1} \underbrace{\sum_{t=0}^{T-1} \tilde{x}(t+K-1-k) e^{-i2\pi f t/T - 1}}_{T_k(f)}. \tag{14}$$

For  $T_k(f)$ , given  $FFT\{x(t-a)\} = X(f)e^{-i2\pi fa/T-1}$ , we have:

$$T_{k}(f) = \sum_{t=0}^{T-1} \tilde{x}(t+K-1-k)e^{-i2\pi f t/T-1}$$

$$= \sum_{t=0}^{T-1} x(t+\frac{K}{2}-k-2)e^{-i2\pi f t/T-1}$$

$$= FFT\{x(t+\frac{K}{2}-k-2)\}$$

$$= X(f)e^{i2\pi f(\frac{K}{2}-k-2)/T-1}$$
(15)

So, we have the Fourier transform of  $\hat{x}(t)$  and its spectral energy:

$$\hat{X}(f) = X(f) - \frac{\beta}{K} \sum_{k=0}^{K-1} X(f) e^{i2\pi f(\frac{K}{2} - k - 2)/T - 1}$$

$$= X(f) \left[ 1 - \beta \cdot \underbrace{\frac{1}{K} \sum_{k=0}^{K-1} e^{i2\pi f(\frac{K}{2} - k - 2)/T - 1}}_{G(f)} \right],$$

$$E_{\hat{X}}(f) = |X(f)|^2 \left\{ 1 - \beta \cdot \underbrace{\frac{1}{K} \sum_{k=0}^{K-1} e^{i2\pi f(\frac{K}{2} - k - 2)/T - 1}}_{G(f)} \right\}^2$$

$$= |X(f)|^2 (1 - \beta \cdot G(f))^2. \tag{16}$$

In this paper, we set K=25 (i.e., T/4+1, T=96), and the function graph of G(f) is shown in Figure 7.

It is evident that G(f) is a gradually decay function, with its values decreasing **from 1 to 0**. This ensures that  $E_{\hat{X}}(f) = |X(f)|^2 (1 - \beta \cdot G(f))^2$ , where, relative to  $E_X$ , the low-frequency components are attenuated, and the mid-frequency components are enhanced.

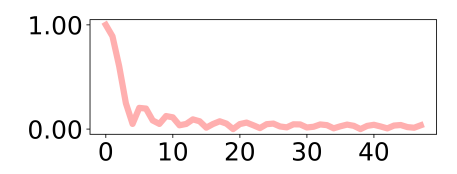


Figure 7: The function G(f) is plotted for T=96 and K=25. Due to the symmetry of the FFT, we only need to plot the values for  $f=0,1,\ldots,48$ .

#### **B** EXPERIMENTAL DETAILS

#### **B.1** Dataset Statistics

We elaborate on the datasets employed in this study with the following details.

- ETT Dataset (Zhou et al., 2022a) comprises two sub-datasets: ETTh and ETTm, which were collected from electricity transformers. Data were recorded at 15-minute and 1-hour intervals for ETTm and ETTh, respectively, spanning from July 2016 to July 2018.
- **Solar\_Energy** (Lai et al., 2018) records the solar power production of 137 PV plants in 2006, which are sampled every 10 minutes.
- **Electricity Dataset**<sup>2</sup> encompasses the electricity consumption data of 321 customers, recorded on an hourly basis, covering the period from 2012 to 2014.
- Traffic Dataset<sup>3</sup> consists of hourly data from the California Department of Transportation.
   It describes road occupancy rates measured by various sensors on San Francisco Bay area freeways.
- Weather Dataset<sup>4</sup> contains records of 21 meteorological indicators, updated every 10 minutes throughout the entire year of 2020.

We follow the same data processing and train-validation-test set split protocol used in iTransformer (Liu et al., 2024b), where the train, validation, and test datasets are strictly divided according to chronological order to make sure there are no data leakage issues. We fix the input length as T=96 for all datasets, and the forecasting length  $F\in\{96,192,336,720\}$ . The characteristics of these datasets are shown in Table 4

Table 4: The Statistics of the eight datasets used in our experiments.

Datasets	ETTh1&2	ETTm1&2	Traffic	Electricity	Solar_Energy	Weather
Variates	7	7	862	321	137	21
Timesteps	17,420	69,680	17,544	26,304	52,560	52,696
Granularity	1 hour	5 min	1 hour	1 hour	10 min	10 min

#### B.2 IMPLEMENTATION DETAILS AND MODEL PARAMETERS

We trained our ReFocus model using the MSE loss function and employed the ADAM optimizer. For evaluation purposes, we used two key performance metrics: the mean square error (MSE) and the mean absolute error (MAE). We initialized the random seed as rs=2024 and set the hyperparameter K=25-kernel size of the convolution kernel in AMEO. The dimension of the Layer is set to D=512 and Q=128. The batch size bs=32 for the Traffic dataset due to its large channel will cause **out of memory** when employed with large batch size, and bs=128 for others. The learning rate is searched from  $lr \in \{1e-5, 1e-4\}$  except for the Traffic dataset (lr=5e-4). The number of EKPB is searched from  $N \in \{1,2,3,4\}$ , and hyperparameter  $\beta$ . which controls the scale magnitude, from  $\beta \in \{0.01,0.1,0.5,1.0\}$ . Our implementation was carried out in PyTorch and

<sup>&</sup>lt;sup>2</sup>https://archive.ics.uci.edu/ml/datasets/ElectricityLoadDiagrams20112014

<sup>3</sup>https://pems.dot.ca.gov/

<sup>4</sup>https://www.bgc-jena.mpg.de/wetter/

executed on a single NVIDIA GeForce RTX 4090 with 24G VRAM. To foster reproducibility, we make our code, and training scripts available in this **Anonymous Repo**<sup>5</sup>.

All the compared multivariate forecasting baseline models that we reproduced are implemented based on the benchmark of **Time series Lab** (Wang et al., 2024d) Repository <sup>6</sup>, which is fairly built on the configurations provided by each model's original paper or official code. Those that have not yet been included in **Time series Lab** are directly reproduced from their official code repositories. It is worth noting that both the baselines used in this paper and our **ReFocus** have fixed a long-standing bug. This bug was originally identified in Informer (Zhou et al., 2022a) (**AAAI 2021 Best Paper**) and subsequently addressed by FITS (Xu et al., 2024b). For specific details about the bug and its resolution, please refer to **GitHub Repository**<sup>7</sup>.

# C FURTHER ANALYSIS OF THE PROPOSED KEY-FREQUENCY ENHANCED TRAINING STRATEGY

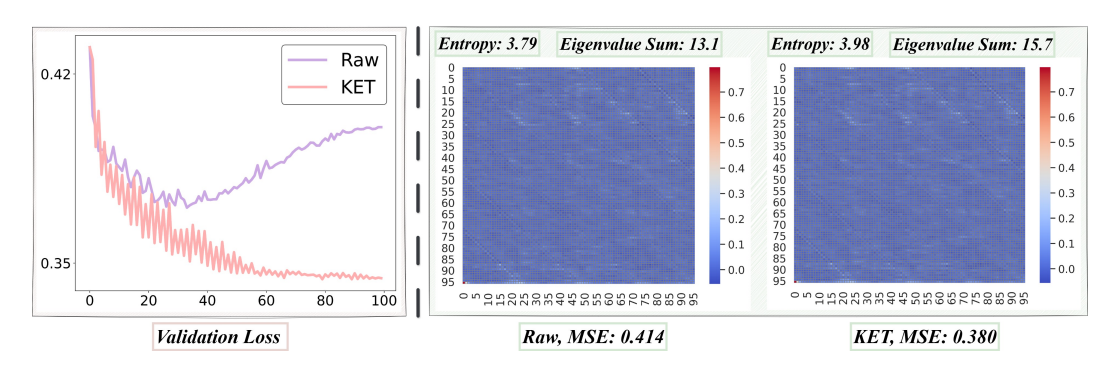


Figure 8: We select the input-96-forecast-96 task on Traffic and visualize the validation loss and weight of our **ReFocus** model. **LEFT**: Visualization of the **Validation Loss** during 100 training epochs with (**KET**) and without KET (**Raw**). **RIGHT**: Visualization about the Weight (Obtained using the approach outlined in **Analysis of linear model** (Toner & Darlow, 2024)) of the trained model. Two significant metrics for assessing the information richness of the weight matrix-the information **Entropy** and the **Sum of Eigenvalues**-are calculated. Both indicate higher quality with greater values.

To further investigate the impact of the proposed 'Key-Frequency Enhanced Training (KET) strategy' on model training and forecasting ability, we visualize its training process regarding Validation Loss and the model weights obtained after training in Figure 8. We also compute the Entropy and the Sum of Eigenvalues of the weight matrix.

The results show that, in the absence of KET, the model quickly overfits around the **24**th epoch, exhibiting poor generalization. In contrast, with the aid of KET, the model consistently performs better on the validation set, converging smoothly without overfitting, and the training process becomes more stable. Additionally, weight visualization results indicate that the model trained with KET has higher information **Entropy** and a greater **Sum of Eigenvalues**, suggesting that the trained model possesses a stronger capacity for feature representation extraction. The predictive results further validate this, as our KET improves the MSE from 0.414 to 0.380, achieving an **8.2%** reduction.

#### D ABLATION STUDY OF DIFFERENT KEY-FREQUENCY PICKING STRATEGY

We conducted an ablation study on various key-frequency selection strategies. The evaluated methods include Maximum-based, Minimum-based, and **Softmax-based** random sampling strategies. Our experimental results in Table 5 reveal that purely relying on Maximum or Minimum-based strategies may overlook certain critical Key-Frequency. In contrast, the random sampling strategy based on a Softmax probabilistic distribution consistently achieved the best overall performance, particularly on

<sup>5</sup>https://anonymous.4open.science/r/ReFocus-2889/

<sup>6</sup>https://github.com/thuml/Time-Series-Library

<sup>7</sup>https://github.com/VEWOXIC/FITS

Table 5: Ablation study of different Key-Frequency Picking strategies. 'Softmax' means using softmax function to generate a probability distribution and picking shared Key-Frequency using this distribution. 'Max' means always choosing the biggest energy. 'Min' means always choosing the smallest energy. We list the average results. Full results are in Appendix K.4.

Picking Strategy	ETTm1	ETTm2	ETTh1	ETTh2	ECL	Traffic	Weather	Solar_Energy
	MSE MAE	MSE MAE	MSE MAE	MSE MAE	MSE MAE	MSE MAE	MSE MAE	MSE MAE
Min	0.388 0.392	0.280 0.323	0.432 0.432	0.371 0.396	0.194 0.281	0.517 0.344	0.378 0.363	0.240 0.270
								0.230 0.260
Softmax	<b>0.387</b> 0.394	0.275 0.320	0.434 0.433	0.371 0.396	0.168 0.262	0.412 0.265	0.346 0.339	0.222 0.252

datasets with a larger number of channels and higher complexity—key challenges in multivariate time series forecasting.

# E COMPARISON OF EKPB AND OTHER INTER-SERIES DEPENDENCIES MODELING BACKBONE

Table 6: Multivariate forecasting result of 'Energy-based Key-Frequency Picking Block' (EKPB) and other inter-series dependencies modeling backbones. We use prediction lengths  $F \in \{96, 192, 336, 720\}$ , and input length T = 96. The best results are in **bold**.

M	odel	EK	PB	iTrans	former	TSM	lixer	Cross	former	FEC	CAM
M	etric	MSE	MAE	MSE	MAE	MSE	MAE	MSE	MAE	MSE	MAE
	96	0.179	0.260	0.180	0.264	0.182	0.266	0.287	0.366	0.188	0.275
72	192	0.244	0.301	0.250	0.309	0.249	0.309	0.414	0.492	0.265	0.336
$\Xi$	336	0.303	0.339	0.311	0.348	0.309	0.347	0.597	0.542	0.318	0.362
回	720	0.401	0.395	0.412	0.407	0.416	0.408	1.730	1.042	0.416	0.417
	Avg	0.282	0.324	0.288	0.332	0.289	0.333	0.757	0.610	0.297	0.348
	96	0.288	0.338	0.297	0.349	0.319	0.361	0.745	0.584	0.298	0.345
걸	192	0.374	0.391	0.380	0.400	0.402	0.410	0.877	0.656	0.377	0.397
	336	0.414	0.426	0.428	0.432	0.444	0.446	1.043	0.731	0.425	0.434
ÌЦ	720	0.421	0.440	0.427	0.445	0.441	0.450	1.104	0.763	0.432	0.450
	Avg	0.374	0.399	0.383	0.407	0.401	0.417	0.942	0.684	0.383	0.407
П	96	0.166	0.209	0.174	0.214	0.166	0.210	0.158	0.230	0.182	0.242
her	192	0.216	0.256	0.221	0.254	0.215	0.256	0.206	0.277	0.223	0.281
Weather	336	0.274	0.296	0.278	0.296	0.287	0.300	0.272	0.335	0.270	0.320
≱	720	0.351	0.346	0.358	0.349	0.355	0.348	0.398	0.418	0.338	0.374
	Avg	0.252	0.277	0.258	0.279	0.256	0.279	0.259	0.315	0.253	0.304
П	96	0.146	0.240	0.148	0.240	0.157	0.260	0.219	0.314	0.178	0.267
اد	192	0.161	0.254	0.162	0.253	0.173	0.274	0.231	0.322	0.185	0.273
Ö	336	0.178	0.273	0.178	0.269	0.192	0.295	0.246	0.337	0.199	0.290
_	720	0.220	0.306	0.225	0.317	0.223	0.318	0.280	0.363	0.235	0.323
	Avg	0.176	0.268	0.178	0.270	0.186	0.287	0.244	0.334	0.199	0.288

Table 6 presents the full results of 'Energy-based Key-Frequency Picking Block (EKPB)' and other inter-series dependency modeling backbones on multivariate time series forecasting tasks. We compared 'Energy-based Key-Frequency Picking Block' (EKPB) with several well-established backbones, including iTransformer (Liu et al., 2024b), TSMixer (Chen et al., 2023), and Crossformer (Zhang & Yan, 2023), which have demonstrated exceptional performance in modeling inter-series dependencies. Additionally, we included FECAM (Jiang et al., 2023), a method also designed for modeling cross-channel frequency-domain dependencies. The results presented in Table 6 demonstrate that our EKPB outperforms in modeling inter-series dependencies across multiple datasets.

# F ABLATION STUDY OF DIFFERENT FREQUENCY PROCESSING STRATEGY

In Table 7, the performance of AMEO on two prediction tasks across two datasets consistently surpasses the results achieved by methods based on RevIN and Filters. Furthermore, while Filters and

Table 7: Experiment result of high-pass filter, low-pass filter, RevIN, and AMEO using a simple linear **projection** as the forecaster on Weather and ETTm1 dataset. We set the input length T=96 and forecasting length  $F \in \{720, 96\}$ .

Dataset	Length	'	IEO		vIN	Lo			gh	None	
		MSE	MAE	MSE	MAE	MSE	MAE	MSE	MAE	MSE	MAE
ETTm1	96	0.331	0.365 0.440	0.354	0.375	0.345	0.371	1.097	0.792	0.348	0.375
EIIIII											
Weather	96	0.164	0.236 0.370	0.194	0.234	0.198	0.258	0.636	0.608	0.198	0.258
weamer	720	0.331	0.370	0.365	0.353	0.353	0.387	0.638	0.611	0.352	0.386

RevIN occasionally lead to degraded performance on certain datasets, AMEO consistently delivers results that outperform the original methods. These findings further highlight the superiority of AMEO over alternative approaches.

#### G VISUALIZATION OF MULTIVARIATE CORRELATIONS

In addition to the main results, we further provide visualizations of multivariate correlations on the Traffic datasets, as shown in Figure 9 (**LEFT**). We calculate the value of the correlation map by:

$$\bar{x}_{i,:} = \frac{1}{T} \sum_{t=1}^{T} x_{i,t}, \quad \tilde{x}_{i,t} = x_{i,t} - \bar{x}_{i,:},$$

$$\tilde{\rho}_{ij} = \frac{\sum_{t=1}^{T} \tilde{x}_{i,t} \, \tilde{x}_{j,t}}{\sqrt{\sum_{t=1}^{T} \tilde{x}_{i,t}^{2}} \sqrt{\sum_{t=1}^{T} \tilde{x}_{j,t}^{2}} + \epsilon}, \quad \epsilon = 1 \times 10^{-8},$$

$$\cot_{ij} = \frac{\exp(\tilde{\rho}_{ij})}{\sum_{k=1}^{N} \exp(\tilde{\rho}_{ik})}.$$
(17)

These results demonstrate that ReFocus effectively captures inter-series dependencies. Moreover, the encoder layer built based on the 'Energy-based Frequency Picking Block' (EKPB) exhibits highly interpretable feature maps. Notably, in the shallow layers, the correlation maps of the learned representation closely resemble the input sequence X, while in deeper layers, the representations progressively align with the target outputs Y. This suggests that ReFocus progressively transforms input features toward task-relevant representations, enabling both effective modeling and interpretability.

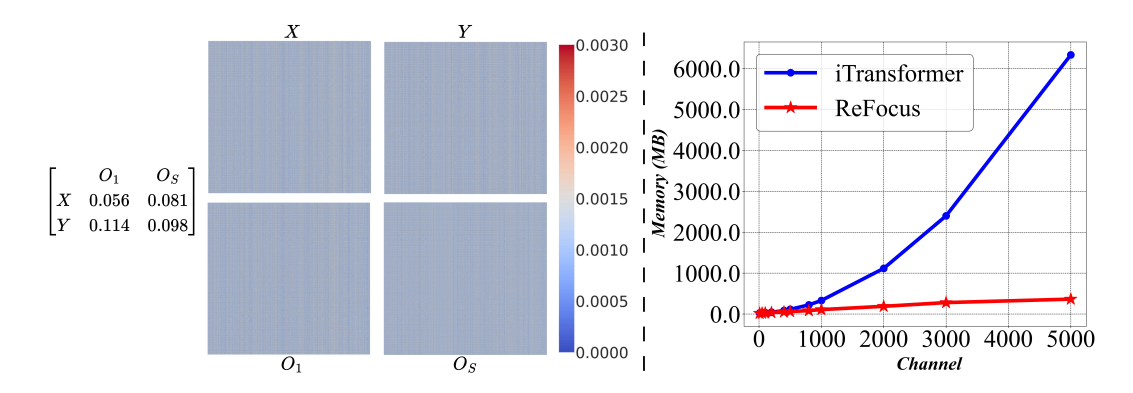


Figure 9: Left: Visualization of multivariate correlations of raw time series (X, Y) and the learned embedding.  $O_1$  is the output embedding of the first encoder block, and  $O_S$  the last. We use the Frobenius norm  $||A - B||_F = \sqrt{\sum_{i,j} (A_{ij} - B_{ij})^2}$  to quantify the similarity. The lower, the higher. **Right**: Memory Usage comparison of ReFocus and iTransformer. We compare the memory consumption under varying numbers of channels (with B = 4, T = 96, F = 720).

# H COMPLEXITY ANALYSIS OF REFOCUS

We analyze the complexity of the ReFocus Encoder concerning the Dimension of model D, number of channels N, dimension of 'Energy-based Frequency Picking Block' (EKPB) Q. The complexity of input MLP is  $O(N \cdot D^2) + O(N \cdot D \cdot Q)$ . Since  $Q \ll D$  (Q = 128, D = 512 in this work), the dominant cost is  $O(N \cdot D^2)$ . During EKPB, the complexity of FFT is  $O(N \cdot Q \cdot \log Q)$ , and so is the IFFT. Complexity of Energy computing, Softmax and Component Picking, each part is  $O(N \cdot Q)$ . Map the representation back to the original space:  $O(N \cdot D \cdot Q)$ . So the overall complexity is  $O(N \cdot D \cdot Q)$ , which is negligible compared to  $O(N \cdot D^2)$ . Each later FFN has  $O(N \cdot D^2)$  complexity. So, the overall complexity of ReFocus Encoder is dominated by  $O(N \cdot D^2)$ , which is Linear to input token number N.

On the other hand, a standard Transformer encoder has complexity  $O(N^2 \cdot D) + O(N \cdot D^2)$  (Self-Attention + FFN). For large N, the Quadradic  $O(N^2)$  term becomes the bottleneck, whereas our **ReFocus** Block avoids this quadratic cost.

As shown in Figure 9 (**RIGHT**), we compare the memory consumption of ReFocus and iTransformer under varying numbers of channels. **ReFocus** exhibits high efficiency, achieving SOTA performance with significantly reduced memory usage and computational cost.

Table 8: Model efficiency analysis. We evaluated the **parameter count**, and the **inference time** (average of 5 runs on a single NVIDIA 4090 24GB GPU) with  $batch\_size = 1$  on **ECL** dataset. We set the dimension of layer  $dim \in \{256, 512\}$ , and the number of network layers N = 2. The task is **input-96-forecast-720**. \* means 'former.' **Para** means 'Parameter count(M).' **Time** means 'inference time(ms).'

Dim	EK	PB	Cı	oss*	iTi	rans*	TSN	Mixer	FE	CAM
	Param	Time	Para	Time	Para	Time	Para	Time	Para	Time
256 512	0.29 0.97	68.91 84.54	0.93 1.78	98.37 118.29	1.27	192.12 249.60	13.66 43.04	432.40 507.54	1.39 5.14	205.66 277.43

Additionally, when comparing the number of parameters and inference time during prediction under identical configurations on the ECL dataset, our EKPB method still outperforms other inter-series dependencies modeling baselines by a significant margin, as in Table 8.

#### I SENSITIVITY OF HYPERPARAMETERS

Table 9: Sensitivity to mixing coefficient in KET ( $\alpha$ ). Since we don't know in advance which two channels share the same frequency information and their correlation intensity, in our work, we choose to use  $\alpha$  sampled from a Normal Distribution to simulate such correlation. Here, we design three ablation methods: w/o means  $\alpha = 0$ , Normal is our default design, and Constant denotes  $\alpha = 1$ .

Dataset	w/o	Normal	Constant
ETTm2	0.402/0.396	0.395/0.392	0.399/0.394
Weather	0.350/0.346	0.344/0.343	0.349/0.346

Table 10: Sensitivity to augmentation intensity ( $\beta$ ) in AMEO.

Dataset	0.0	0.2	0.4	0.6	0.8	1.0
ETTm2	0.398	0.397	0.397	0.397	0.397	<b>0.396</b> 0.348
Weather	0.349	0.348	<b>0.346</b>	<b>0.346</b>	0.347	

We studied the sensitivity of **ReFocus** to four major hyperparameters: the mixing coefficient in KET  $(\alpha, \text{Table } 9)$ , the augmentation intensity parameter  $(\beta, \text{Table } 10)$ , the kernel size (K, Table 11) in AMEO, and the number of encoder layers (N, Table 12). Results of MSE on ETTm2 and Weather datasets are reported.

Table 11: Sensitivity to kernel size (K) in AMEO.

Dataset	7	15	25	51	75
ETTm2 Weather	0.000	0.399 <b>0.346</b>	0.396 0.346	0.07	0.397 0.349

Table 12: Sensitivity to the number of encoder layers (N).

Dataset	1	2	3	4	5
ETTm2 Weather	0.00	0.397 0.346	0.00	0.398 <b>0.344</b>	0.398 0.348

#### J EXTENDED DISCUSSION AND EVALUATION

#### J.1 Broader Discussion on the Mid-Frequency Gap

Although we only demonstrated the mid-frequency gap on energy, traffic, and weather benchmarks, this phenomenon is well-documented in many other domains. In econometrics, financial time series exhibit spectra dominated by very low frequencies with a mid-band "valley" that simple filters cannot remedy (Stock & Watson, 2002; Granger & Newbold, 1974). In biomedical signals such as EEG, negligible mid-frequency energy in resting-state recordings is commonly reported (Chatfield & Xing, 2019; Niedermeyer & da Silva, 2005). Similar patterns were also observed in human activity recognition (HAR) signals, where energy is concentrated in low-frequency bands while the mid-frequency region remains nearly empty (Anguita et al., 2013; Lara & Labrador, 2012).

To validate the broader applicability of ReFocus, we extended experiments to classification tasks in Medical time series and HAR. Following Medformer (Wang et al., 2024c), we evaluate on APAVA (EEG dataset) and UCI-HAR benchmarks, both known to exhibit mid-frequency gaps. Baselines include Medformer (Wang et al., 2024c), iTransformer (Liu et al., 2024b), and PatchTST (Nie et al., 2023), using Accuracy and F1-score as metrics. Results in Table 13 confirm the effectiveness of ReFocus across these tasks.

Table 13: Classification results on APAVA and UCI-HAR datasets.

Dataset	Metric	ReFocus (Ours)	Medformer	iTransformer	PatchTST
APAVA	Accuracy F1-score	82.61 81.88	78.74 76.31	74.55 72.30	67.03 55.97
UCI-HAR	Accuracy F1-score	93.17 93.27	91.65 91.61	92.41 92.39	87.67 88.02

#### J.2 SHORT-TERM TIME SERIES FORECASTING

We conducted experiments on the M4 benchmark to test the generalizability of ReFocus on short-term time series forecasting. Following the protocol of TimesNet (Wu et al., 2023), we compare against TimesNet (Wu et al., 2023), PatchTST (Nie et al., 2023), DLinear (Zeng et al., 2023), and Autoformer (Wu et al., 2021). Performance is reported with SMAPE, MASE, and OWA (lower is better). As shown in Table 14, ReFocus consistently achieves the best overall results across yearly, quarterly, and monthly tasks, further affirming its robustness in modeling complex temporal variations.

These extended evaluations demonstrate the broad applicability and robustness of our approach beyond the original long-term time series forecasting tasks.

Table 14: Forecasting results on the M4 dataset. Lower SMAPE/MASE/OWA is better.

Category	Metric	ReFocus (Ours)	TimesNet	PatchTST	DLinear	Autoformer
Yearly	SMAPE	13.201	13.387	16.463	16.965	13.974
	MASE	2.912	2.996	3.967	4.283	3.134
	OWA	0.778	0.786	1.003	1.058	0.822
Quarterly	SMAPE	9.964	10.100	10.644	12.145	11.338
	MASE	1.162	1.182	1.278	1.520	1.365
	OWA	0.873	0.890	0.949	1.106	1.012
Monthly	SMAPE	12.541	12.670	13.399	13.514	13.958
	MASE	0.914	0.933	1.031	1.037	1.103
	OWA	0.862	0.878	0.949	0.956	1.002

#### K FULL RESULTS

 The full experiment results are provided in the following section due to the space limitation of the main text.

#### K.1 FULL MULTIVARIATE FORECASTING RESULTS

Table 15 contains the detailed results of Ten baselines and our ReFocus on eight well-acknowledged forecasting benchmarks. ReFocus consistently achieves the best overall performance across all datasets, especially in tasks with a large number of channels, such as the Solar\_Energy dataset (137 channels), ECL dataset (321 channels), and Traffic dataset (862 channels). It obtains the best performance in terms of MSE: 34 out of 40 tasks, and MAE: 36 out of 40 tasks. These results demonstrate the outstanding performance of ReFocus in multivariate time series forecasting tasks.

#### K.2 FULL RESULTS OF ABLATION ON AMEO AND KET

Table 16 presents the full results of the ablation study on 'Adaptive Mid-Frequency Energy Optimizer (AMEO)' and 'Key-Frequency Enhanced Training (KET)'. KET and AMEO contribute significantly to the model's performance, each providing substantial improvements. Moreover, their combination further enhances the model, achieving peak performance. These results provide strong evidence of the effectiveness of both AMEO and KET.

# K.3 FULL RESULTS OF FURTHER ABLATION STUDY ON KET

Table 17 exhibits the full results of a further ablation study on the 'Key-Frequency Enhanced Training (KET)' strategy. Introducing Pseudo samples—obtained by randomly incorporating spectral information from other channels into the current channel—generally leads to performance improvement. However, on more complex datasets, it results in performance degradation. In contrast, alternating training between Real and Pseudo samples (**Our KET**) overcomes this issue, yielding a further and consistent enhancement in performance.

# K.4 FULL RESULTS OF ABLATION STUDY OF DIFFERENT KEY-FREQUENCY PICKING STRATEGIES

Table 18 illustrates the complete results of the ablation study on various Key-Frequency Picking strategies. Notably, our **Softmax-based random sampling** strategy consistently achieves the best overall performance, particularly on more complex datasets.

Table 15: Multivariate long-term forecasting result comparison. We use prediction lengths  $F \in \{96, 192, 336, 720\}$ , and input length T = 96. The best results are in **bold**, and the second best are <u>underlined</u>.

N	/Iodel	ReFocus			er ModernTCN			Crossformer		TSMixer	DLinear	FreTS
		(Ours)	(2024)	(2024b)	(2024)	(2024b)	(2023)	(2023)	(2023)	(2023)	(2023)	(2023c)
N	/letric	MSE MAE	MSE MAE	MSE MA	E MSE MAE	MSE MAE	MSE MAE	MSE MAE	MSE MAE	MSE MAE	MSE MAE	MSE MAE
_	96	1		-!	0.317 0.362	1	1	0.404 0.426				
ETTm1	192 336	1		1	0.366 0.389 0.407 0.412	1		0.450 0.451 0.532 0.515		l.		1
EŢ	720				9 0.466 0.443	1						
	Avg	<del></del>			0 0.389 0.402		! —					<u> </u>
	96				4 0.173 0.255							
2	192			0.250 0.30		·	1	0.414 0.492				
ETTm2	336				8 0.308 0.344		1	0.597 0.542				1
回	720	0.395 0.392	0.414 0.405	0.412 0.40	7 <u>0.398</u> <u>0.394</u>	0.407 0.399	0.402 0.400	1.730 1.042	0.408 0.403	0.416 0.408	0.554 0.522	0.495 0.480
	Avg	0.275 0.320	0.285 0.328	0.288 0.33	2 0.279 0.322	0.286 0.328	0.281 0.326	0.757 0.610	0.291 0.333	0.289 0.333	0.350 0.401	0.321 0.368
	96	0.376 0.394	0.382 0.402	0.386 0.40	5 0.386 0.394	0.386 0.396	0.414 0.419	0.423 0.448	0.384 0.402	0.401 0.412	0.386 0.400	0.395 0.407
ĮĮ.	192				6 0.436 0.423		·I	0.471 0.474				
ETTh1	336	1		1	8 0.479 0.445		1	!				1
۳	720	0.470 0.474	<u>0.481</u> 0.473	0.503 0.49	1 0.481 <u>0.469</u>	0.502 0.495	0.500 0.488	0.653 0.621	0.521 0.500	0.507 0.490	0.519 0.516	0.558 0.532
	Avg	0.434 0.433	<u>0.441</u> 0.439	0.454 0.44	7 0.446 <u>0.433</u>	0.451 0.440	0.469 0.454	0.529 0.522	0.458 0.450	0.463 0.452	0.456 0.452	0.475 0.463
	96	0.288 0.337	0.293 0.343	0.297 0.34	9 0.292 0.340	0.295 0.350	0.302 0.348	0.745 0.584	0.340 0.374	0.319 0.361	0.333 0.387	0.309 0.364
Jh2	192	0.371 0.390				·	1	0.877 0.656				
ETTh2	336				2 0.424 0.434							
۳1	720	0.417 0.436	0.449 0.460	0.427 0.44	0.433 0.448	0.431 0.446	0.431 0.446	1.104 0.763	0.462 0.468	0.441 0.450	0.831 0.657	0.721 0.604
	Avg	0.371 0.396	0.383 0.407	0.383 0.40	7 0.382 0.404	0.383 0.408	0.387 0.407	0.942 0.684	0.414 0.427	0.401 0.417	0.559 0.515	0.472 0.465
	96	1			0.173 0.260	1	1	1		l .		
ECL	192			1	3 0.181 0.267	1	1	1		l .		
핆	336			-1	0.196 0.283	1	1	l				
	720			-1	7 0.238 0.316							
	Avg	0.168 0.262	0.173 0.268	0.178 0.27	0.197 0.282							
	96	0.380 0.248			-	1	1	0.522 0.290				
Traffic	192				0.527 0.337							
Tra	336 720	1			3 0.537 0.342 2 0.570 0.359	1	1	1		l .		
					- 1	1						<u> </u>
_	Avg				2 0.546 0.348							
	96			1	4 0.165 <u>0.203</u>	.	1	1		l .		
मू	192 336				4 0.212 <b>0.247</b> 6 0.266 0.293	1	1	l				
Weather	720			-1	9 0.344 0.343	1	1	l				1
<i>&gt;</i>	Avg				9 0.247 0.272							
<u>اح</u>	96		<u> </u>	- <u>1</u>	7 0.206 0.264							<u> </u>
erg	192	0.182 0.219			-	1	1	0.734 0.725		l.		
펿	336	0.240 0.268				1	I	0.750 0.735				
Solar_Energy	720	1			0.264 0.298	1	1	1				1
$^{\circ}$	Avg	0.222 0.252	0.243 0.283	0.233 0.26	2 0.244 0.286	0.395 0.407	0.270 0.307	0.641 0.639	0.301 0.319	0.260 0.297	0.330 0.401	0.248 0.296
	1 <sup>st</sup> Count		2 2	0 0	1 2	0 0	1 0	2 0	0 0	0 0	0 0	0 0
		1 22 20		1	1 - 2	1 " "	1 "	1 - 1		1 1		

Table 16: Full result of ablation study on the 'Adaptive Mid-Frequency Energy Optimizer (AMEO)' and the 'Key-Frequency Enhanced Training (KET)' strategy. We use prediction lengths  $F \in \{96, 192, 336, 720\}$ , and input length T=96. The best results are in **bold**.

	1.1								
M	odel	Both (	ReFocus)	+ Al	MEO	+ K	ET	No	one
Me	etric	MSE	MAE	MSE	MAE	MSE	MAE	MSE	MAE
	96	0.321	0.360	0.331	0.368	0.331	0.363	0.339	0.367
n T	192	0.365	0.379	0.377	0.390	0.373	0.382	0.381	0.391
£	336	0.398	0.400	0.403	0.407	0.403	0.402	0.414	0.413
Ш	720	0.463	0.437	0.462	0.441	0.467	0.438	0.468	0.442
	Avg	0.387	0.394	0.393	0.402	0.394	0.396	0.401	0.403
	96	0.173	0.255	0.179	0.262	0.178	0.260	0.180	0.262
m2	192	0.237	0.297	0.244	0.304	0.241	0.299	0.245	0.302
Ē	336	0.295	0.334	0.304	0.340	0.300	0.337	0.304	0.340
Щ	720	0.395	0.392	0.402	0.396	0.398	0.393	0.404	0.396
	Avg	0.275	0.320	0.282	0.326	0.279	0.322	0.283	0.325
	96	0.376	0.394	0.382	0.398	0.378	0.395	0.383	0.395
μŢ	192	0.428	0.422	0.433	0.425	0.432	0.423	0.432	0.425
L	336	0.462	0.442		0.450				
Ш	720	0.470	0.474	0.489	0.486	0.470	0.474	0.474	0.480
	Avg	0.434	0.433	0.443	0.440	0.437	0.435	0.440	0.437
$\Box$	96	0.288	0.337	0.285	0.336	0.289	0.339	0.288	0.338
h2	192	0.371	0.390	0.375	0.391	0.374	0.390	0.374	0.391
H	336	0.409	0.421	0.405	0.420	0.412	0.425	0.419	0.428
Ш	720	0.417	0.436	0.424	0.441	0.418	0.438	0.423	0.441
	Avg	0.371	0.396	0.372	0.397	0.373	0.398	0.376	0.400
	96	0.143	0.238		0.241				
		0.158	0.252		0.259				
E	336	0.172	0.267		0.272				
	720	0.198	0.290	0.206	0.297	0.203	0.292	0.221	0.307
	Avg	0.168	0.262	0.174	0.267	0.171	0.263	0.178	0.270
	96	0.380	0.248	0.414	0.274	0.380	0.250	0.414	0.278
ЭIJ	192	0.403	0.259	0.439	0.287	0.404	0.262	0.437	0.284
raf	336	0.419	0.267	1	0.288				
П	720	0.446	0.287	0.506	0.307	0.450	0.290	0.495	0.307
	Avg	0.412	0.265	0.452	0.289	0.414	0.268	0.449	0.289
٠	96	0.160	0.202	1	0.209	1			
the		0.211	0.248	1	0.252			1	
/eal	336	0.266	0.290	1	0.291				
	720	0.344	0.343	0.350	0.346	0.349	0.345	0.353	0.349
	Avg	0.245	0.271	0.248	0.275	0.250	0.275	0.252	0.278
rgy	96	0.182	0.219	0.197	0.226	0.192	0.230	0.192	0.234
olar_Energy	192	0.222	0.249	0.236	0.269	0.231	0.255	0.235	0.265
	336	0.240	0.268	0.246	0.276	0.244	0.271	0.249	0.279
	720	0.242	0.271	0.245	0.274	0.245	0.274	0.250	0.278
 \\S	Avg	0.222	0.252	0.231	0.261	0.228	0.258	0.232	0.264

Table 17: Full result of further ablation study on the 'Key-Frequency Enhanced Training (KET)' strategy. We use prediction lengths  $F \in \{96, 192, 336, 720\}$ , and input length T = 96. The best results are in **bold**.

Model Both (KET)	M. I.I. p. gram, p p										
96											
192	M	etric	MSE	MAE	MSE	MAE	MSE	MAE			
Avg   0.394   0.396   0.398   0.401   0.403     Avg   0.394   0.396   0.396   0.398   0.401   0.403     Avg   0.394   0.396   0.396   0.398   0.401   0.403     Avg   0.241   0.299   0.242   0.299   0.245   0.302     336   0.300   0.337   0.301   0.339   0.304   0.340     Avg   0.279   0.322   0.280   0.323   0.283   0.325     336   0.469   0.447   0.467   0.445   0.469   0.449     720   0.470   0.474   0.467   0.472   0.474   0.480     Avg   0.437   0.435   0.436   0.434   0.440   0.437     Avg   0.373   0.398   0.370   0.390   0.374   0.391     336   0.412   0.425   0.412   0.423   0.423   0.423   0.424     Avg   0.373   0.398   0.370   0.397   0.376   0.400     Avg   0.171   0.263   0.165   0.257   0.162   0.256     336   0.417   0.269   0.179   0.271   0.180   0.274     720   0.460   0.269   0.179   0.271   0.180   0.274     720   0.450   0.290   0.454   0.299   0.449   0.288     720   0.349   0.345   0.352   0.275   0.266   0.178   0.269     720   0.349   0.345   0.352   0.275   0.265   0.363   0.394     Avg   0.414   0.268   0.417   0.271   0.449   0.288     720   0.349   0.345   0.352   0.275   0.299     720   0.349   0.345   0.352   0.275   0.299     720   0.349   0.345   0.352   0.246   0.255   0.216   0.256     336   0.273   0.295   0.253   0.276   0.252   0.278     4vg   0.215   0.252   0.216   0.255   0.216   0.256     336   0.273   0.295   0.275   0.297   0.275   0.299     720   0.349   0.345   0.352   0.346   0.353   0.347     Avg   0.215   0.252   0.216   0.255   0.216   0.256     336   0.273   0.295   0.275   0.297   0.275   0.299     720   0.349   0.345   0.352   0.266   0.353   0.244     Avg   0.244   0.271   0.287   0.301   0.249   0.279     720   0.349   0.345   0.353   0.245   0.250   0.231   0.245   0.247     720   0.245   0.275   0.253   0.276   0.252   0.278     720   0.349   0.345   0.250   0.308   0.250   0.278     720   0.349   0.345   0.250   0.308   0.250   0.278     720   0.349   0.345   0.296   0.308   0.250   0.278     720   0.349   0.345   0.296   0.308   0.250   0.278     720		96	0.331	0.363	0.331	0.362	0.339	0.367			
Avg   0.394   0.396   0.398   0.401   0.408   0.442     Avg   0.394   0.396   0.396   0.398   0.401   0.403     P6   0.178   0.260   0.178   0.260   0.180   0.262     192   0.241   0.299   0.242   0.299   0.245   0.302     336   0.300   0.337   0.301   0.339   0.304   0.340     Avg   0.279   0.322   0.280   0.323   0.283   0.325     P6   0.378   0.395   0.382   0.394   0.383   0.395     336   0.469   0.447   0.467   0.445   0.469   0.449     720   0.470   0.474   0.467   0.472   0.474   0.480     Avg   0.437   0.435   0.436   0.434   0.440   0.437     P6   0.289   0.339   0.370   0.390   0.374   0.391     336   0.412   0.425   0.412   0.423   0.419   0.428     720   0.418   0.438   0.418   0.437   0.423   0.441     Avg   0.373   0.398   0.372   0.397   0.376   0.400     P6   0.145   0.239   0.147   0.241   0.147   0.242     192   0.161   0.253   0.165   0.257   0.162   0.256     336   0.476   0.269   0.179   0.271   0.180   0.274     720   0.450   0.290   0.454   0.299   0.495   0.307     Avg   0.414   0.262   0.406   0.265   0.437   0.288     720   0.450   0.290   0.454   0.297   0.275   0.299     720   0.349   0.345   0.352   0.275   0.299   0.295   0.221   0.307     Avg   0.215   0.252   0.216   0.255   0.216   0.256     336   0.273   0.295   0.275   0.297   0.275   0.299     720   0.349   0.345   0.352   0.366   0.353   0.347     Avg   0.250   0.275   0.253   0.276   0.252   0.278     P6   0.164   0.207   0.166   0.207   0.164   0.209     192   0.215   0.252   0.216   0.255   0.216   0.256     336   0.273   0.295   0.275   0.297   0.275   0.299     720   0.349   0.345   0.353   0.245   0.249   0.279     720   0.349   0.345   0.353   0.245   0.249   0.279     720   0.349   0.345   0.253   0.266   0.250   0.245   0.278     P6   0.192   0.230   0.235   0.266   0.255   0.276   0.252   0.278     P7   700   0.349   0.345   0.296   0.308   0.250   0.278     P8   0.192   0.230   0.235   0.266   0.250   0.245   0.278     P8   0.192   0.230   0.235   0.266   0.250   0.245   0.250   0.245   0.250   0.245   0.250   0	m1										
Avg   0.394   0.396   0.396   0.398   0.401   0.403     P6	TT										
Per   Per	Щ	720	0.467	0.438	0.471	0.440	0.468	0.442			
192   0.241   0.299   0.242   0.299   0.245   0.302     336   0.300   0.337   0.301   0.339   0.304   0.340     Avg   0.279   0.322   0.280   0.323   0.283   0.325     96   0.378   0.395   0.382   0.394   0.383   0.395     192   0.432   0.423   0.429   0.423   0.432   0.425     336   0.469   0.447   0.467   0.445   0.469   0.449     720   0.470   0.474   0.467   0.472   0.474   0.480     Avg   0.437   0.390   0.370   0.390   0.374   0.391     336   0.412   0.425   0.412   0.423   0.423   0.419   0.428     720   0.418   0.438   0.418   0.437   0.423   0.441     Avg   0.373   0.398   0.372   0.397   0.376   0.400     96   0.145   0.239   0.147   0.241   0.147   0.242     192   0.161   0.253   0.165   0.257   0.162   0.256     336   0.176   0.269   0.179   0.271   0.180   0.274     720   0.203   0.292   0.209   0.296   0.221   0.307     Avg   0.171   0.263   0.175   0.266   0.178   0.270     Avg   0.414   0.262   0.406   0.265   0.447   0.288     720   0.450   0.290   0.454   0.293   0.495   0.307     Avg   0.414   0.268   0.417   0.271   0.449   0.288     720   0.349   0.345   0.352   0.216   0.255   0.216   0.256     336   0.273   0.295   0.275   0.297   0.275   0.299     720   0.349   0.345   0.352   0.346   0.353   0.347     Avg   0.250   0.275   0.253   0.276   0.252   0.278     Avg   0.250   0.275   0.253   0.276   0.252   0.278     Avg   0.250   0.275   0.253   0.276   0.252   0.278     Avg   0.250   0.275   0.253   0.263   0.192   0.234     Avg   0.244   0.271   0.287   0.301   0.249   0.279     336   0.244   0.271   0.287   0.301   0.249   0.279     337   0.245   0.275   0.296   0.308   0.250   0.278     338   0.245   0.274   0.296   0.308   0.250   0.278     340   0.245   0.274   0.296   0.308   0.250   0.278     340   0.245   0.274   0.296   0.308   0.250   0.278     340   0.245   0.274   0.296   0.308   0.250   0.278     340   0.245   0.274   0.296   0.308   0.250   0.278     340   0.245   0.274   0.296   0.308   0.250   0.278     340   0.245   0.274   0.296   0.308   0.250   0.278     340   0.245		Avg	0.394	0.396	0.396	0.398	0.401	0.403			
Avg   0.374   0.390   0.370   0.390   0.304   0.340     Avg   0.279   0.322   0.280   0.323   0.283   0.325     96   0.378   0.395   0.382   0.394   0.383   0.395     192   0.432   0.423   0.429   0.423   0.432   0.425     336   0.469   0.447   0.467   0.445   0.469   0.449     720   0.470   0.474   0.467   0.472   0.474   0.480     Avg   0.437   0.435   0.436   0.434   0.440   0.437     96   0.289   0.339   0.288   0.338   0.288   0.338     192   0.374   0.390   0.370   0.390   0.374   0.391     336   0.412   0.425   0.412   0.423   0.419   0.428     720   0.418   0.438   0.418   0.437   0.423   0.441     Avg   0.373   0.398   0.372   0.397   0.376   0.400     96   0.145   0.239   0.147   0.241   0.147   0.242     192   0.161   0.253   0.165   0.257   0.162   0.256     336   0.176   0.269   0.179   0.271   0.180   0.274     720   0.203   0.292   0.209   0.296   0.221   0.307     Avg   0.171   0.263   0.175   0.266   0.178   0.270     Avg   0.414   0.262   0.406   0.265   0.437   0.284     336   0.421   0.270   0.424   0.272   0.449   0.288     720   0.450   0.290   0.454   0.293   0.495   0.307     Avg   0.414   0.268   0.417   0.271   0.449   0.288     96   0.164   0.207   0.166   0.207   0.164   0.209     192   0.215   0.252   0.216   0.255   0.216   0.256     336   0.273   0.295   0.275   0.297   0.275   0.299     720   0.349   0.345   0.352   0.346   0.353   0.347     Avg   0.250   0.275   0.253   0.276   0.252   0.278     20   0.192   0.230   0.235   0.263   0.192   0.234     192   0.244   0.271   0.287   0.301   0.249   0.279     192   0.245   0.274   0.296   0.308   0.250   0.278     20   0.245   0.274   0.296   0.308   0.250   0.278     30   0.245   0.274   0.296   0.308   0.250   0.278     30   0.245   0.274   0.296   0.308   0.250   0.278     30   0.244   0.271   0.296   0.308   0.250   0.278     30   0.244   0.271   0.296   0.308   0.250   0.278     30   0.245   0.274   0.296   0.308   0.250   0.278     30   0.245   0.274   0.296   0.308   0.250   0.278     30   0.245   0.274   0.296   0.308   0.	_,										
Avg   0.373   0.399   0.393   0.404   0.396     Avg   0.279   0.322   0.280   0.323   0.283   0.325     96   0.378   0.395   0.382   0.394   0.383   0.395     192   0.432   0.423   0.429   0.423   0.425   0.426   0.445     720   0.470   0.474   0.467   0.445   0.469   0.449     Avg   0.437   0.435   0.436   0.434   0.440   0.437     96   0.289   0.339   0.288   0.338   0.288   0.338     192   0.374   0.390   0.370   0.390   0.374   0.391     336   0.412   0.425   0.412   0.423   0.419   0.428     720   0.418   0.438   0.418   0.437   0.423   0.441     Avg   0.373   0.398   0.372   0.397   0.376   0.400     96   0.145   0.239   0.147   0.241   0.147   0.242     192   0.161   0.253   0.165   0.257   0.162   0.256     336   0.176   0.269   0.179   0.271   0.180   0.274     720   0.203   0.292   0.209   0.296   0.221   0.307     Avg   0.171   0.263   0.175   0.266   0.178   0.270     Avg   0.414   0.262   0.406   0.265   0.449   0.288     720   0.450   0.290   0.454   0.293   0.495   0.307     Avg   0.414   0.268   0.417   0.271   0.449   0.289     96   0.164   0.207   0.166   0.207   0.164   0.209     192   0.215   0.252   0.216   0.255   0.216   0.256     336   0.273   0.295   0.275   0.297   0.275   0.299     720   0.349   0.345   0.352   0.346   0.353   0.347     Avg   0.250   0.275   0.253   0.276   0.252   0.278     20   30   0.244   0.271   0.287   0.301   0.249   0.279     192   0.245   0.255   0.290   0.303   0.235   0.265     336   0.244   0.271   0.287   0.301   0.249   0.279     336   0.421   0.255   0.290   0.303   0.235   0.265     336   0.273   0.295   0.235   0.263   0.192   0.234     336   0.244   0.271   0.287   0.301   0.249   0.279     336   0.244   0.271   0.287   0.301   0.249   0.279     337   0.296   0.308   0.250   0.278     338   0.244   0.271   0.287   0.301   0.249   0.279     338   0.244   0.271   0.287   0.301   0.249   0.279     338   0.244   0.271   0.296   0.308   0.250   0.278     340   0.245   0.274   0.296   0.308   0.250   0.278	'n										
Avg   0.279   0.322   0.280   0.323   0.283   0.325     96   0.378   0.395   0.382   0.394   0.383   0.395     192   0.432   0.423   0.429   0.423   0.425   0.425     336   0.469   0.447   0.467   0.445   0.469   0.449     720   0.470   0.474   0.467   0.472   0.474   0.480     Avg   0.437   0.390   0.388   0.338   0.288   0.338     192   0.374   0.390   0.370   0.390   0.374   0.391     336   0.412   0.425   0.412   0.423   0.419   0.428     720   0.418   0.438   0.418   0.437   0.423   0.441     Avg   0.373   0.398   0.372   0.397   0.376   0.400     96   0.145   0.239   0.147   0.241   0.147   0.242     192   0.161   0.253   0.165   0.257   0.162   0.256     336   0.176   0.269   0.179   0.271   0.180   0.274     720   0.203   0.292   0.209   0.296   0.221   0.307     Avg   0.171   0.263   0.175   0.266   0.178   0.270     Avg   0.414   0.262   0.406   0.265   0.437   0.284     336   0.421   0.270   0.424   0.272   0.449   0.288     720   0.450   0.290   0.454   0.293   0.495   0.307     Avg   0.414   0.268   0.417   0.271   0.449   0.289     96   0.164   0.207   0.166   0.207   0.164   0.209     192   0.215   0.252   0.216   0.255   0.216   0.256     336   0.273   0.295   0.275   0.297   0.275   0.299     720   0.349   0.345   0.352   0.346   0.353   0.347     Avg   0.250   0.275   0.253   0.276   0.252   0.278     20   30   0.244   0.271   0.287   0.301   0.249   0.279     192   0.245   0.255   0.290   0.303   0.235   0.265     336   0.244   0.271   0.287   0.301   0.249   0.279     336   0.244   0.271   0.287   0.301   0.249   0.279     336   0.244   0.271   0.287   0.301   0.249   0.279     337   0.296   0.308   0.250   0.278	II										
Part	Щ	720	0.398	0.393	0.399	0.393	0.404	0.396			
192		Avg	0.279	0.322	0.280	0.323	0.283	0.325			
Avg   0.437   0.447   0.467   0.445   0.469   0.449     Avg   0.437   0.435   0.436   0.434   0.440   0.437     96   0.289   0.339   0.288   0.338   0.288   0.338     192   0.374   0.390   0.370   0.390   0.374   0.391     336   0.412   0.425   0.412   0.423   0.419   0.428     720   0.418   0.438   0.418   0.437   0.423   0.441     Avg   0.373   0.398   0.372   0.376   0.400     192   0.161   0.253   0.165   0.257   0.162   0.254     720   0.203   0.292   0.209   0.296   0.221   0.307     Avg   0.171   0.263   0.175   0.266   0.178   0.270     Avg   0.414   0.268   0.417   0.271   0.449   0.288     192   0.404   0.262   0.496   0.265   0.437   0.284     336   0.421   0.270   0.424   0.272   0.449   0.288     192   0.404   0.262   0.406   0.265   0.437   0.284     336   0.421   0.270   0.424   0.271   0.449   0.289     192   0.215   0.252   0.216   0.255   0.216   0.256     336   0.273   0.295   0.275   0.297   0.275   0.299     720   0.349   0.345   0.352   0.346   0.353   0.347     Avg   0.250   0.275   0.253   0.276   0.252   0.278     240   0.192   0.230   0.235   0.263   0.192   0.234     192   0.231   0.255   0.290   0.303   0.249   0.279     192   0.231   0.255   0.290   0.303   0.249   0.279     192   0.231   0.255   0.290   0.303   0.249   0.279     193   0.244   0.271   0.287   0.301   0.249   0.279     194   0.245   0.274   0.296   0.308   0.250   0.278     195   0.245   0.274   0.296   0.308   0.250   0.278     196   0.192   0.230   0.235   0.263   0.249   0.279     197   0.245   0.274   0.296   0.308   0.250   0.278     198   0.244   0.271   0.287   0.301   0.249   0.279     199   0.245   0.274   0.296   0.308   0.250   0.278     190   0.245   0.274   0.296   0.308   0.250   0.278     190   0.245   0.274   0.296   0.308   0.250   0.278     190   0.245   0.274   0.296   0.308   0.250   0.278     190   0.245   0.274   0.296   0.308   0.250   0.278     190   0.245   0.274   0.296   0.308   0.250   0.278     190   0.245   0.274   0.296   0.308   0.250   0.278     190   0.245   0.247   0.296   0.308											
Avg   0.437   0.438   0.436   0.434   0.440   0.437     96   0.289   0.339   0.288   0.338   0.288   0.338     192   0.374   0.390   0.370   0.390   0.374   0.391     336   0.412   0.425   0.412   0.423   0.419   0.428     720   0.418   0.438   0.418   0.437   0.423   0.441     Avg   0.373   0.398   0.372   0.397   0.376   0.400     192   0.161   0.253   0.147   0.241   0.147   0.242     192   0.161   0.253   0.150   0.257   0.162   0.256     336   0.176   0.269   0.179   0.271   0.180   0.274     720   0.203   0.292   0.209   0.296   0.221   0.307     Avg   0.411   0.263   0.175   0.266   0.178   0.270     4vg   0.414   0.262   0.406   0.265   0.437   0.284     336   0.421   0.270   0.424   0.272   0.449   0.288     720   0.450   0.290   0.454   0.293   0.495   0.307     Avg   0.414   0.268   0.417   0.271   0.449   0.289     192   0.215   0.252   0.216   0.255   0.216   0.256     336   0.273   0.295   0.275   0.297   0.275   0.299     720   0.349   0.345   0.352   0.346   0.353   0.347     Avg   0.250   0.275   0.253   0.276   0.252   0.278     20   0.231   0.255   0.290   0.303   0.235   0.265     336   0.244   0.271   0.287   0.301   0.249   0.279     192   0.231   0.255   0.290   0.303   0.249   0.279     192   0.231   0.255   0.290   0.303   0.249   0.279     192   0.245   0.274   0.296   0.308   0.250   0.278	Th1										
Avg   0.437   0.435   0.436   0.434   0.440   0.437     96   0.289   0.339   0.288   0.338   0.288   0.338     192   0.374   0.390   0.370   0.390   0.374   0.391     336   0.412   0.425   0.412   0.423   0.419   0.428     720   0.418   0.438   0.418   0.437   0.423   0.441     Avg   0.373   0.398   0.372   0.397   0.376   0.400     192   0.161   0.253   0.165   0.257   0.162   0.256     336   0.176   0.269   0.179   0.271   0.180   0.274     720   0.203   0.292   0.209   0.296   0.221   0.307     Avg   0.171   0.263   0.175   0.266   0.178   0.270     Avg   0.414   0.262   0.406   0.265   0.437   0.284     336   0.421   0.270   0.424   0.272   0.449   0.288     720   0.450   0.290   0.454   0.293   0.495   0.307     Avg   0.414   0.268   0.417   0.271   0.449   0.289     192   0.215   0.252   0.216   0.255   0.216   0.256     336   0.273   0.295   0.275   0.297   0.275   0.299     720   0.349   0.345   0.352   0.346   0.353   0.347     Avg   0.250   0.275   0.253   0.276   0.252   0.278     20   0.231   0.255   0.290   0.303   0.235   0.265     336   0.244   0.271   0.287   0.301   0.249   0.279     336   0.244   0.271   0.287   0.301   0.249   0.279     336   0.244   0.271   0.287   0.301   0.249   0.279     336   0.244   0.271   0.287   0.301   0.249   0.279     336   0.244   0.271   0.287   0.301   0.249   0.279     336   0.244   0.271   0.287   0.301   0.249   0.279     336   0.244   0.271   0.287   0.301   0.249   0.279     337   0.245   0.274   0.296   0.308   0.250   0.278     338   0.244   0.271   0.287   0.301   0.249   0.279     338   0.244   0.271   0.287   0.301   0.249   0.279     338   0.244   0.271   0.287   0.301   0.249   0.279     336   0.244   0.271   0.287   0.301   0.249   0.279     336   0.244   0.271   0.296   0.308   0.250   0.278	E										
Per   Per	Н	720	0.470	0.474	0.467	0.472	0.474	0.480			
192		Avg	0.437	0.435	0.436	0.434	0.440	0.437			
Avg   0.171   0.263   0.412   0.427   0.418   0.428   0.270   0.428   0.270   0.208   0.275   0.266   0.178   0.270   0.450   0.269   0.275   0.266   0.178   0.270   0.450   0.269   0.275   0.266   0.178   0.270   0.203   0.290   0.294   0.210   0.450   0.265   0.450   0.265   0.450   0.265   0.450   0.265   0.450   0.265   0.450   0.265   0.450   0.265   0.450   0.265   0.450   0.265   0.450   0.265		96	0.289	0.339							
Avg   0.171   0.263   0.175   0.266   0.178   0.270     Avg   0.380   0.250   0.383   0.250   0.441   0.249     Avg   0.414   0.262   0.454   0.291   0.366   0.470     Avg   0.164   0.252   0.209   0.296   0.221   0.307     Avg   0.171   0.263   0.175   0.266   0.178   0.270     Avg   0.404   0.262   0.406   0.265   0.437   0.284     336   0.421   0.270   0.424   0.272   0.449   0.288     720   0.450   0.290   0.454   0.293   0.495   0.307     Avg   0.171   0.268   0.417   0.271   0.449   0.289     Avg   0.215   0.252   0.216   0.255   0.216   0.256     336   0.273   0.295   0.275   0.297   0.275   0.299     720   0.349   0.345   0.352   0.346   0.353   0.347     Avg   0.250   0.275   0.253   0.276   0.252   0.278     Avg   0.250   0.275   0.253   0.276   0.252   0.278     Avg   0.244   0.271   0.287   0.301   0.249   0.279     Avg   0.244   0.271   0.287   0.301   0.249   0.279     Avg   0.244   0.271   0.287   0.301   0.249   0.279     Avg   0.245   0.274   0.296   0.308   0.250   0.278     Avg   0.265   0.274   0.296	'n2	192	0.374								
Avg   0.373   0.398   0.372   0.397   0.376   0.400     96	H										
96	щ	720	0.418	0.438	0.418	0.437	0.423	0.441			
192   0.161   0.253   0.165   0.257   0.162   0.256   0.176   0.269   0.179   0.271   0.180   0.274   0.203   0.292   0.209   0.296   0.221   0.307     Avg   0.171   0.263   0.175   0.266   0.178   0.270     96   0.380   0.250   0.383   0.254   0.414   0.278   0.404   0.262   0.406   0.265   0.437   0.284   0.450   0.450   0.290   0.454   0.293   0.495   0.307     Avg   0.414   0.268   0.417   0.271   0.449   0.289   0.215   0.252   0.216   0.255   0.216   0.255   0.216   0.255   0.216   0.255   0.216   0.255   0.216   0.256   0.347   0.349   0.345   0.352   0.346   0.353   0.347     Avg   0.250   0.275   0.253   0.276   0.252   0.278   0.252   0.278   0.253   0.235   0.265   0.244   0.271   0.287   0.301   0.249   0.279   0.245   0.244   0.271   0.287   0.301   0.249   0.279   0.245   0.278   0.296   0.308   0.250   0.278   0.250   0.278   0.250   0.278   0.266   0.308   0.250   0.278   0.250   0.250   0.278   0.250   0.250   0.278   0.250   0.250   0.278   0.250   0.250   0.278   0.250   0.250   0.278   0.250   0.250   0.250   0.278   0.250   0.250   0.278   0.250   0.250   0.278   0.250		Avg	0.373	0.398	0.372	0.397	0.376	0.400			
Avg   0.171   0.263   0.175   0.266   0.178   0.270     Avg   0.171   0.263   0.175   0.266   0.178   0.270     Avg   0.380   0.250   0.383   0.254   0.414   0.278     192   0.404   0.262   0.406   0.265   0.437   0.284     720   0.450   0.290   0.454   0.293   0.495   0.307     Avg   0.414   0.268   0.417   0.271   0.449   0.289     192   0.215   0.252   0.216   0.255   0.216   0.256     336   0.273   0.295   0.275   0.253   0.216   0.256     336   0.273   0.295   0.275   0.253   0.216   0.256     336   0.274   0.255   0.253   0.276   0.252   0.278     20   0.349   0.345   0.353   0.245   0.234     20   0.231   0.255   0.290   0.303   0.235   0.265     336   0.244   0.271   0.287   0.301   0.249   0.279     336   0.244   0.271   0.287   0.301   0.249   0.279     336   0.244   0.271   0.287   0.301   0.249   0.279     336   0.244   0.271   0.287   0.301   0.249   0.279     336   0.244   0.271   0.287   0.301   0.249   0.279     336   0.244   0.271   0.287   0.301   0.249   0.279     336   0.244   0.271   0.287   0.301   0.249   0.279     337   0.245   0.274   0.296   0.308   0.250   0.278     338   0.244   0.271   0.296   0.308   0.250   0.278     339   0.245   0.274   0.296   0.308   0.250   0.278     340   0.245   0.274   0.296   0.308   0.250   0.278		96	0.145	0.239			l				
	П	192	0.161	0.253							
Avg   0.171   0.263   0.175   0.266   0.178   0.270     96	EC										
96   0.380   0.250   0.383   0.254   0.414   0.278   0.404   0.262   0.406   0.265   0.437   0.284   0.424   0.270   0.424   0.272   0.449   0.288   720   0.450   0.290   0.454   0.293   0.495   0.307   0.450   0.290   0.454   0.293   0.495   0.307   0.460   0.265   0.275   0.216   0.255   0.216   0.255   0.216   0.255   0.216   0.255   0.216   0.255   0.216   0.256   0.273   0.295   0.275   0.297   0.275   0.299   0.349   0.345   0.353   0.347   0.250   0.275   0.253   0.276   0.252   0.278   0.253   0.275   0.299   0.234   0.231   0.255   0.290   0.303   0.235   0.265   0.246   0.279   0.245   0.245   0.278   0.296   0.308   0.250   0.250   0		720	0.203	0.292	0.209	0.296	0.221	0.307			
192   0.404   0.262   0.406   0.265   0.437   0.284     336   0.421   0.270   0.424   0.272   0.449   0.288     720   0.450   0.290   0.454   0.293   0.495   0.307     Avg   0.414   0.268   0.417   0.271   0.449   0.289     192   0.215   0.252   0.216   0.255   0.216   0.256     336   0.273   0.295   0.275   0.297   0.275   0.299     720   0.349   0.345   0.352   0.346   0.353   0.347     Avg   0.250   0.275   0.253   0.276   0.252   0.278     202   0.231   0.255   0.290   0.303   0.235   0.265     336   0.244   0.271   0.287   0.301   0.249   0.279     336   0.244   0.271   0.287   0.301   0.249   0.279     336   0.244   0.271   0.287   0.301   0.249   0.278     337   0.245   0.278   0.296   0.308   0.250   0.278     338   0.244   0.271   0.296   0.308   0.250   0.278     339   0.245   0.274   0.296   0.308   0.250   0.278     330   0.245   0.274   0.296   0.308   0.250   0.278     330   0.245   0.274   0.296   0.308   0.250   0.278     330   0.245   0.278   0.296   0.308   0.250   0.278     330   0.245   0.274   0.296   0.308   0.250   0.278     330   0.245   0.278   0.296   0.308   0.250   0.278     330   0.245   0.278   0.296   0.308   0.250   0.278     330   0.245   0.278   0.296   0.308   0.250   0.278     330   0.245   0.278   0.296   0.308   0.250   0.278     330   0.245   0.278   0.296   0.308   0.250   0.278     330   0.245   0.274   0.296   0.308   0.250   0.278     330   0.245   0.274   0.296   0.308   0.250   0.278     330   0.245   0.274   0.296   0.308   0.250   0.278     330   0.245   0.245   0.245   0.245   0.245   0.245     330   0.245   0.245   0.245   0.245   0.245   0.245   0.245     330   0.245		Avg	0.171	0.263	0.175	0.266	0.178	0.270			
Avg   0.414   0.268   0.417   0.271   0.449   0.289     Avg   0.414   0.268   0.417   0.271   0.449   0.289     192   0.215   0.252   0.216   0.255   0.216   0.256     336   0.273   0.295   0.275   0.297   0.275   0.299     720   0.349   0.345   0.352   0.346   0.353   0.347     Avg   0.250   0.275   0.253   0.276   0.252   0.278     192   0.231   0.255   0.290   0.303   0.235   0.265     192   0.231   0.255   0.290   0.303   0.249   0.279     193   0.244   0.271   0.287   0.301   0.249   0.279     194   0.245   0.274   0.296   0.308   0.250   0.278		96	0.380	0.250							
Avg   0.414   0.268   0.417   0.271   0.449   0.289     96	Яc	192	0.404	0.262							
Avg   0.414   0.268   0.417   0.271   0.449   0.289     192   0.215   0.252   0.216   0.255   0.216   0.256     336   0.273   0.295   0.275   0.297   0.275   0.299     720   0.349   0.345   0.352   0.346   0.353   0.347     Avg   0.250   0.275   0.253   0.276   0.252   0.278     202   0.231   0.225   0.290   0.303   0.235   0.265     192   0.244   0.271   0.287   0.301   0.249   0.279     336   0.244   0.271   0.287   0.301   0.249   0.279     720   0.245   0.274   0.296   0.308   0.250   0.278	raf										
96   0.164   0.207   0.166   0.207   0.164   0.209     192   0.215   0.252   0.216   0.255   0.216   0.256     336   0.273   0.295   0.275   0.297   0.275   0.299     720   0.349   0.345   0.352   0.346   0.353   0.347     Avg   0.250   0.275   0.253   0.276   0.252   0.278     192   0.231   0.255   0.290   0.303   0.235   0.265     336   0.244   0.271   0.287   0.301   0.249   0.279     720   0.245   0.274   0.296   0.308   0.250   0.278	L	720	0.450	0.290	0.454	0.293	0.495	0.307			
192   0.215   0.252   0.216   0.255   0.216   0.256   0.273   0.295   0.275   0.297   0.275   0.299   0.349   0.345   0.352   0.346   0.353   0.347     Avg   0.250   0.275   0.253   0.276   0.252   0.278   0.252   0.252   0.278   0.252   0.278   0.252   0.278   0.252   0.278   0.252		Avg	0.414								
336   0.273   0.295   0.275   0.297   0.275   0.299     720   0.349   0.345   0.352   0.346   0.353   0.347     Avg   0.250   0.275   0.253   0.276   0.252   0.278     360   96   0.192   0.230   0.235   0.263   0.192   0.234     192   0.231   0.255   0.290   0.303   0.235   0.265     336   0.244   0.271   0.287   0.301   0.249   0.279     720   0.245   0.274   0.296   0.308   0.250   0.278	ı.										
Avg   0.250   0.275   0.253   0.276   0.252   0.278     Avg   0.250   0.275   0.253   0.276   0.252   0.278     Avg   0.250   0.275   0.253   0.276   0.252   0.278     Avg   0.250   0.275   0.253   0.265   0.290   0.303   0.235   0.265     Avg   0.241   0.255   0.290   0.303   0.235   0.265     Avg   0.244   0.271   0.287   0.301   0.249   0.279     Avg   0.245   0.274   0.296   0.308   0.250   0.278     Avg   0.250   0.274   0.296   0.308   0.250   0.278     Avg   0.250   0.275   0.253   0.276   0.250   0.278     Avg   0.250   0.275   0.253   0.276   0.252   0.278     Avg   0.250   0.275   0.253   0.265   0.278     Avg   0.250   0.250   0.278     Avg   0.250   0.278   0.250   0.278     Avg   0.250   0.274   0.296   0.308   0.250   0.278     Avg   0.250   0.274   0.274   0.276   0.278     Avg   0.250   0.274   0.276   0.278     Avg   0.250   0.278   0.278   0.278     Avg   0.250   0.278   0.278   0.278     Avg   0.250   0.278   0.278   0.278   0.278     Avg   0.250   0.278   0.278   0.278   0.278     Avg   0.250   0.278   0.278   0.278   0.278   0.278     Avg   0.250   0.278   0.278   0.278   0.278   0.278   0.278   0.278     Avg   0.250   0.278   0.278   0.278   0.278   0.278   0.278   0.278   0.278   0.278   0.278   0.278   0.278   0.278   0.278	the										
Avg   0.250   0.275   0.253   0.276   0.252   0.278     50   96   0.192   0.230   0.235   0.263   0.192   0.234     192   0.231   0.255   0.290   0.303   0.235   0.265     336   0.244   0.271   0.287   0.301   0.249   0.279     720   0.245   0.274   0.296   0.308   0.250   0.278	/ea										
192   0.230   0.235   0.263   0.192   0.234   0.255   0.290   0.303   0.235   0.265   0.244   0.271   0.287   0.301   0.249   0.279   0.245   0.274   0.296   0.308   0.250   0.278	>	720	0.349	0.345	0.352	0.346	0.353	0.347			
20   96   0.192   0.230   0.235   0.263   0.192   0.234   0.235   0.265   0.290   0.303   0.235   0.265   0.294   0.271   0.247   0.247   0.248   0.274   0.296   0.308   0.250   0.278   0.288   0.277   0.294   0.232   0.264		Avg	0.250	0.275	0.253	0.276	0.252	0.278			
192   0.231   0.255   0.290   0.303   0.235   0.265     336   0.244   0.271   0.287   0.301   0.249   0.279     720   0.245   0.274   0.296   0.308   0.250   0.278     Avg   0.228   0.258   0.277   0.294   0.232   0.264	rgy										
336   0.244   0.271   0.287   0.301   0.249   0.279	3ne										
Section   720   0.245   0.274   0.296   0.308   0.250   0.278         Avg   0.228   0.258   0.277   0.294   0.232   0.264											
Avg   0.228 0.258   0.277 0.294   0.232 0.264	olaı	720	0.245	0.274	0.296	0.308	0.250	0.278			
	S	Avg	0.228	0.258	0.277	0.294	0.232	0.264			

Table 18: Full result about ablation study of different Key-Frequency Picking strategies. We use prediction lengths  $F \in \{96, 192, 336, 720\}$ , and input length T = 96. The best results are in **bold**.

M	odel	Soft	max	M	ax	M	lin		
M	etric	MSE	MAE	MSE	MAE	MSE	MAE		
	96	0.321	0.360	0.331	0.360	0.321	0.357		
ml	192				0.380				
TT		0.398				l			
Э	720	0.463	0.437	0.467	0.438	0.464	0.436		
	Avg	0.387	0.394	0.392	0.395	0.388	0.392		
	96				0.258	l			
m	192				0.300	l			
TT		0.295				l			
Щ	720	0.395	0.392	0.396	0.392	0.398	0.394		
	Avg	0.275	0.320	0.279	0.322	0.280	0.323		
	96				0.396				
.'h1	192				0.423				
TT	336				0.444				
щ	720	0.470	0.474	0.473	0.478	0.467	0.472		
	Avg	0.434	0.433	0.437	0.435	0.432	0.432		
	96				0.340				
'h2	192				0.391				
TT	336				0.425	l			
щ	720	0.417	0.436	0.418	0.437	0.419	0.437		
	Avg	0.371		l					
	96	l			0.241				
Ţ	192				0.256	1			
EC	336				0.269				
	720	0.198	0.290	0.204	0.293	0.242	0.318		
	Avg	0.168	0.262	0.172	0.265	0.194	0.281		
	96	0.380	0.248	0.389	0.253	0.504	0.341		
Яc	192	0.403							
raf	336				0.276				
L	720	0.446	0.287	0.457	0.296	0.536	0.347		
	Avg	0.412	0.265	0.422	0.273	0.517	0.344		
	96	0.160							
heı	192				0.248				
/eat	336				0.291				
*	720	0.344	0.343	0.348	0.344	0.349	0.344		
	Avg	0.245	0.271	0.249	0.273	0.249	0.272		
gy	96				0.228				
nei	192	0.222							
r_E	336				0.273				
Solar_Energy	720	0.242	0.271	0.248	0.276	0.253	0.280		
S	Avg	0.222	0.252	0.230	0.260	0.240	0.270		

# L LIMITATIONS AND FUTURE WORKS

**Limitations** Despite ReFocus demonstrating significant improvements in multivariate time series forecasting by addressing the mid-frequency spectrum gap and exploiting shared key-frequency information, several limitations remain. First, our experiments primarily rely on benchmark datasets (Traffic, ECL, Solar), which may not capture the full variability of more diverse, high-frequency, or non-stationary applications. Additionally, further analysis is needed to understand the robustness of our approach under abrupt distribution shifts or extreme noise conditions.

**Future Works** Future work should extend the ReFocus framework to a broader range of application domains, such as financial, medical, and human activity time series, to verify its generalizability. We plan to explore adaptive mechanisms to dynamically tune module parameters and mitigate sensitivity issues. Moreover, investigating lightweight or hybrid architectures could improve real-time forecasting efficiency. Incorporating external contextual information may further enrich inter-channel dependency modeling. All these will help refine the overall design and improve resilience against challenging, non-stationary environments.

## M SOCIETAL IMPACTS

 The development of the ReFocus forecaster has the potential to significantly benefit various fields, such as finance and traffic, by improving the accuracy and efficiency of time series forecasting, thereby enhancing decision-making processes. However, there are potential negative societal impacts to consider. Privacy concerns may arise from the use of personal data, especially in healthcare and finance, leading to possible violations. Additionally, biases in the data could result in unfair outcomes, perpetuating existing disparities. Over-reliance on automated forecasting models might lead to the neglect of important context, causing adverse outcomes. To mitigate these risks, robust data protection protocols should be implemented, and continuous monitoring for bias is necessary to ensure fairness. Developing ethical use policies and maintaining human oversight in decision-making can further ensure that the deployment of ReFocus maximizes its positive societal impact while minimizing potential negative consequences.